Introduction to rock properties

MSc Geo-Energy with Machine Learning and Data Science

Professor Matthew Jackson

Department of Earth Science and Engineering

Imperial College London

0. Introduction

This one-day course introduces key rock properties relevant to subsurface geoenergy projects, including CO_2 storage, thermal energy storage, hydrogen storage and geothermal energy production. The acquisition and interpretation of data describing these properties is generally termed 'petrophysics' and the data are described as 'petrophysical data'. Today we will briefly review methods to measure these properties in the laboratory using rock samples ('cores') brought to surface during drilling. This specific branch of petrophysics is termed 'core petrophysics'.

The focus of core petrophysics is to measure properties on rock samples recovered directly from the reservoir. The rock samples tested in core petrophysics are typically cylindrical 'plugs' of rock of two different sizes. Smaller plugs are typically ca. 3-5cm in length and ca. 2.5cm in diameter. Larger plugs are typically ca. 5-8cm in length and ca. 4cm in diameter. These plugs may be directly sampled in the borehole after the borehole is drilled or may be drilled out from larger continuous cores acquired during borehole drilling. Some experiments are conducted directly on the larger continuous cores.

0.1 Key Learning Outcomes

1. Understand concepts of representative elementary volume (REV), porosity, permeability, electrical conductivity, thermal conductivity, specific heat capacity, Darcy's Law, Ohm's Law, Fourier's Law
2. Know how core samples are recovered to the laboratory from the reservoir
3. Know the most common methods used to measure porosity, permeability, electrical conductivity, thermal conductivity, specific heat capacity in the laboratory along with their advantages, disadvantages and limitations

0.2 Course structure

Section 1: Definition and measurement of porosity and permeability

Section 2: Definition and measurement of electrical properties

Section 3: Definition and measurement of thermal properties

Section 4: Core material acquisition and handling

Section 5: Classroom exercises

1. Definition and measurement of porosity and permeability

1.1. Porosity and grain density

1.1.1. Definition of porosity

Porosity is the fraction of the total rock volume that is void space. A typical cylindrical core of rock, with radius R and length L, has an *apparent* or *bulk volume* of $V_b = \pi R^2 L$. Some of this volume is occupied by rock minerals, and some of it is void space (Figure 1.1.1).

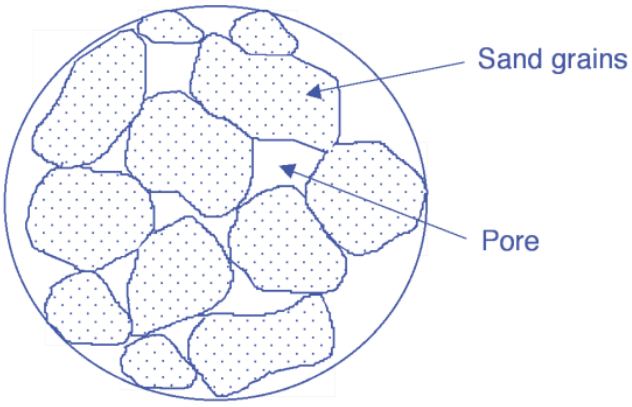

Fig. 1.1.1. Schematic of a porous sandstone, showing grains and pore space. Typical pore sizes are microns to hundreds of microns (one micron = 0.000001m = 0.001mm)

The grain volume of the core, V_g, is the actual volume occupied by mineral grains. The pore volume, V_p, is the volume of the void space. These volumes are related by

$$V_b = V_g + V_p \tag{1.1.1}$$

The fraction of the rock that is occupied by pore space is known as the *porosity*, and is usually denoted by ϕ (although sometimes by n):

$$\phi = V_p / V_b \tag{1.1.2}$$

The porosity may also be expressed as a percentage of the total rock volume, and in a typical reservoir rock can range from a few percent, to as high as 40%.

Porosity is often subdivided into *primary porosity*, which is the porosity that the rock had after it was first deposited and compacted, and *secondary porosity*, which is any porosity that is subsequently created through mineral dissolution, mineral deposition, and fracturing. Another distinction that can be made is between *total porosity*, which is the porosity that is defined by eq. (1.1.2), and *effective porosity*, which measures only the pore space that is interconnected and which can potentially host, and form a flow path, for fluids (Fig. 1.1.2). The total porosity is therefore composed of *effective*/interconnected porosity, and *ineffective*/unconnected porosity.

The ineffective porosity may comprise isolated pores (i.e. pores that are not interconnected), and also connected porosity which contains immobile water (i.e. water that is bound to clay minerals or held in very small pores within clay minerals by capillary forces). Porosity between grains is termed *inter-granular porosity*, while porosity within grains is termed *intra-granular porosity*. Inter-granular porosity typically forms the most significant porosity system for the storage of fluids and is often conceptually modelled as a system of *pores* and *throats* (Fig. 1.1.2); the pores are the larger voids between grains, and the throats are the narrower pathways that connect the pores (or pore-bodies). Typical porosity values are shown in Table 1.1.1.

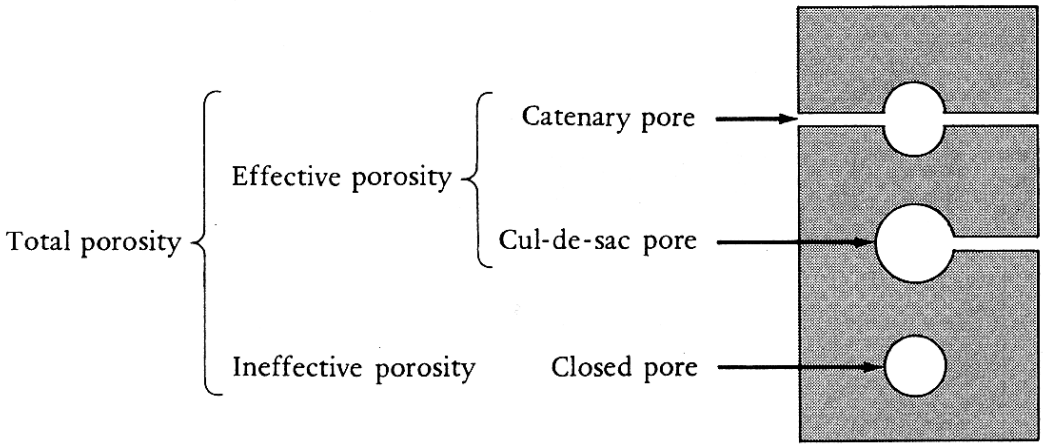

Fig. 1.1.2. Schematic showing effective and ineffective porosity. A catenary pore is connected to more than one other pore. Pores are often thought to be larger voids connected by narrower throats.

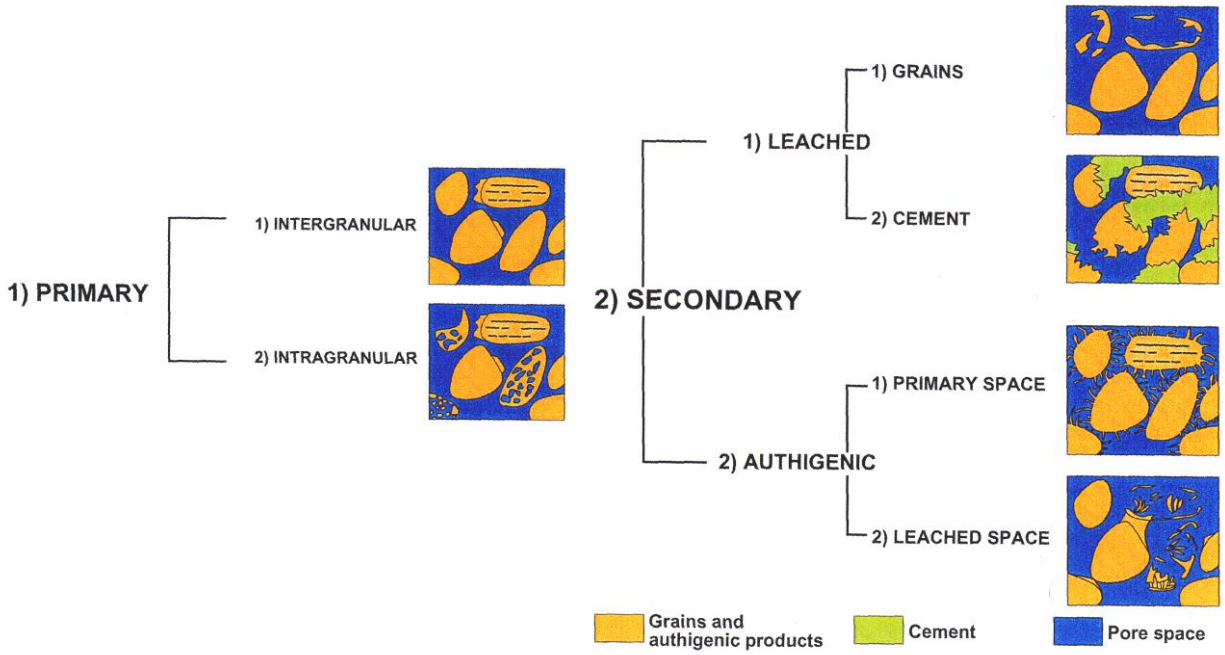

Fig. 1.1.3. Schematic showing primary and secondary porosity. Authigenic refers to a mineral formed where it is found (i.e. in-situ) rather than transported.

Rock Type	Range
Unconsolidated sands	35 - 40%
Sandstones	20 - 35%
Tight/well cemented sandstones	15 - 20%
Limestones	5 - 20%
Dolomites	10 - 30%
Chalk	5 - 40%

Table 1.1.1 Typical porosity values in reservoir rocks

1.1.2. Heterogeneity and the "Representative Elementary Volume"

The property of porosity introduces an issue, that of *heterogeneity*, which is important for all petrophysical properties. To say that a reservoir is heterogeneous, means that its properties vary from point to point. In one sense, all rock masses are heterogeneous because, as we move away from a given rock at a given location, we will eventually encounter a different rock type. For example, some reservoirs contain beds of sandstone and mudstone, with thicknesses on the order of a few meters (e.g. Fig. 1.1.4). These reservoirs are heterogeneous on length scales on the order of tens of meters. Within the sandstones, there may be sedimentary structures such as cross-beds that define heterogeneity at the scale of mm to cm and, within the cross-beds, there may be variations in grain shape, size and packing that define heterogeneity at the order of μm – mm.

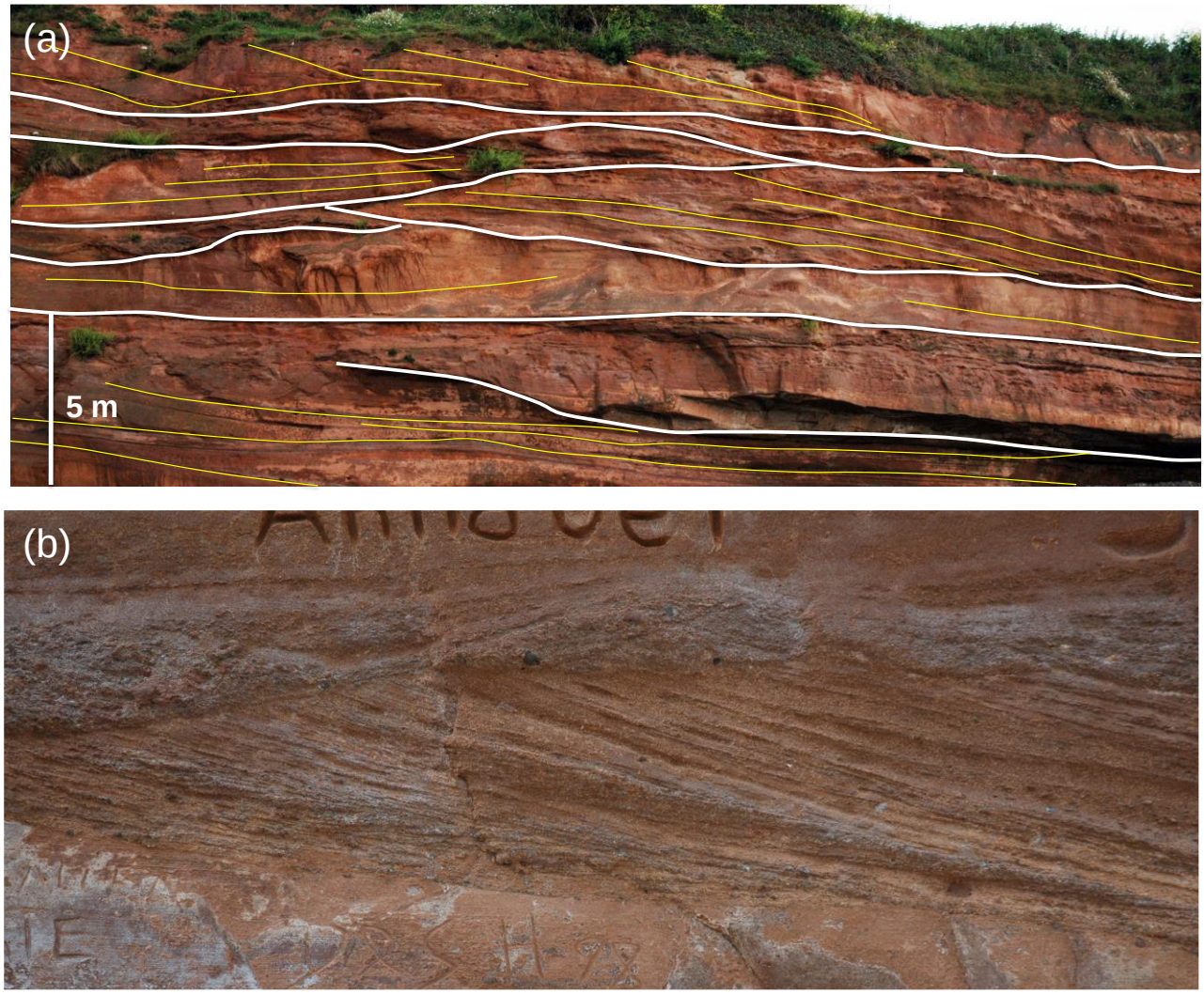

Fig. 1.1.4. Examples of reservoir heterogeneity. (a) Interbedded sandstones and mudstones in the Sherwood sandstone exposed at Sidmouth on the south coast of the UK. (b) Close up of the same unit, exposed at Ladram Bay on the south coast of the UK, showing cross-bedding picked out by subtle variations in grain size.

At the other extreme of length-scale, all porous rocks are heterogeneous on the scale of the pore size. Consider Figure 1.1.5, where x_1 and x_2 are two locations in the rock. The porosity at location x_1 is zero, because point x_1 lies in a sand grain. On the other hand, point x_2 lies in a pore, so, strictly speaking, the porosity at x_2 is 1. Clearly, it makes no sense to talk about the porosity at some infinitely small mathematical point in the reservoir. When we discuss porosity (and other petrophysical properties such as permeability, and electrical and thermal conductivity), we implicitly are referring to the *average* value in some small region.

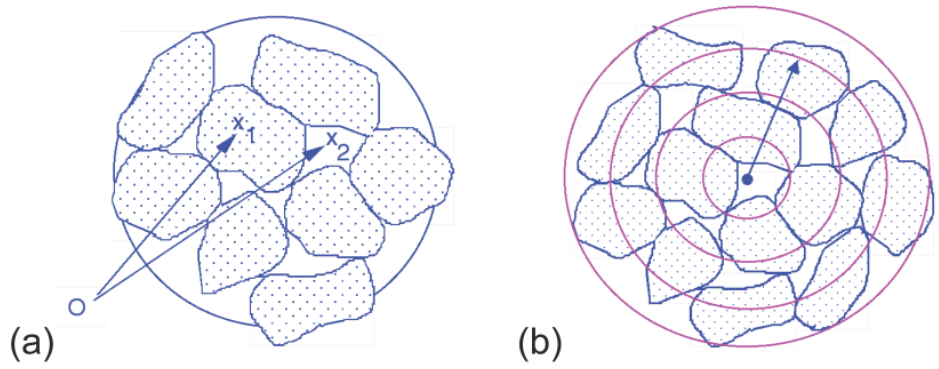

Fig. 1.1.5. (a) Porosity at x_1 is 0, and at x_2 is 1, illustrating that porosity cannot be defined at a point, but over a volume. (b) $\phi(R)$ can be defined as an average over a region of radius R (length of the arrow).

Imagine that we could measure the porosity in a small spherical region of rock, of radius R, surrounding the point x_2, as in Fig. 1.1.5b. This average value is $\phi(R)$. For very small values of R, $\phi(R) = 1$. As R gets larger and the spherical region (or sample volume) encompasses some of the nearby sand grains, $\phi(R)$ will decrease. In a typical sandstone, $\phi(R)$ will fluctuate with R, but eventually stabilize to some constant value. Eventually, as R gets large enough that the sample volume crosses over into the next rock type, $\phi(R)$ might change abruptly. Schematically, we can represent this situation as in Fig 1.1.6.

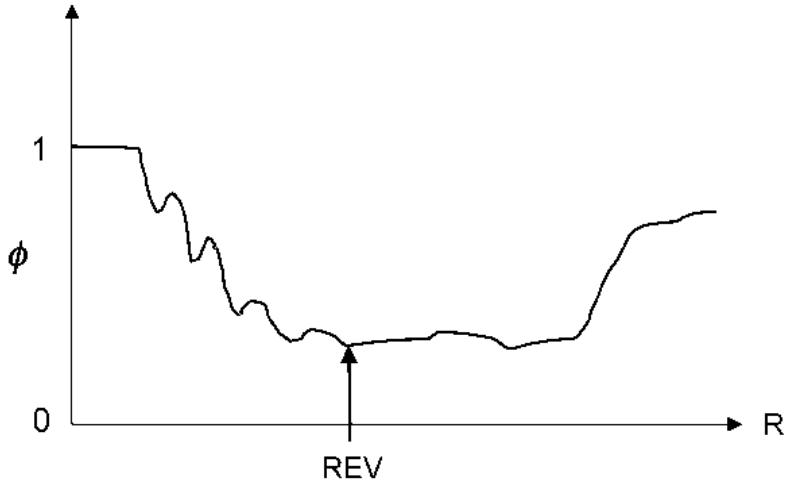

Fig. 1.1.6. Porosity as a function of sample volume, showing the existence of a Representative Elementary Volume (REV).

The minimum value of R that is needed for the porosity to stabilise is known as the 'representative elementary volume' (REV), or the 'representative volume element' (RVE). When we talk about the value of a petrophysical property such as porosity, we are usually implicitly referring to the value as defined on a length-scale at least as large as the REV. For sandstones with a uniform grain size distribution, the REV must be at least about ten grain diameters. However, for heterogeneous rocks such as many carbonates, the REV may be much larger, as heterogeneity may exist at many scales. In fact, there is no guarantee that a REV scale exists for a given rock. But in reservoir characterisation and modelling, we always assume that a REV can be defined, and often assume it corresponds to the length scale of plug measurements in the laboratory, or wireline measurements downhole. This is often a significant over-simplification, as will be discussed later in the course.

1.1.3 Laboratory measurement of porosity

There are several different methods developed for porosity measurements. These methods measure two of three critical parameters: (1) bulk volume V_b, (2) grain volume V_g and (3) pore volume V_p. The third can always be calculated from the two others using equation (1.1.1).

1.1.3.1 Bulk Volume

Although the bulk volume may be computed from measurements of the dimensions of a regularly shaped sample, the usual procedure utilizes Archimedes' principle that the volume of fluid displaced by an immersed body is equal to the volume of the body and measures the bulk volume of the core in a fluid that will not enter the pore-space, such as mercury. This technique is particularly advantageous as it can be applied to irregular-shaped samples. Care must be taken to prevent fluid invasion into the pore space of the rock. Mercury is often used because it is strongly non-wetting in the presence of gas and has a high interfacial tension. However, special care must be taken when applying this technique on vuggy samples (vugs are large pores, typically created by dissolution), since the sample may be contaminated by mercury invasion into the large voids.

1.1.3.2 Grain Volume

The most widely used technique makes use of Boyle's law and is termed the Boyle's law or gas expansion method. Boyle's Law states that

'*The absolute pressure exerted by a given mass of an ideal gas is inversely proportional to the volume it occupies if the temperature remains unchanged within a closed system*.'

This method involves the expansion of a compressed gas (usually helium, owing to its small molecular size, low adsorption onto rock surfaces, and close to ideal behaviour at relatively low pressure) into a clean, dry sample. A schematic of Boyle's law porosimeter is shown in Figure 1.1.7.

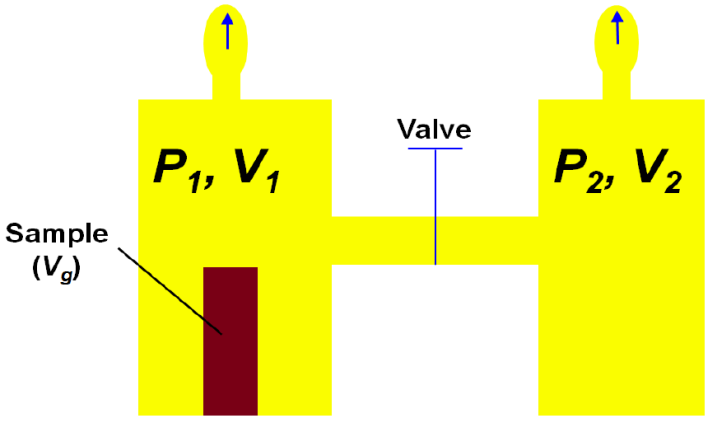

Figure 1.1.7 Schematic of the double-cell Boyle's law porosimeter.

Gas (helium) is initially admitted to the reference cell of known volume V_2 at a pre-set reference pressure P_2. The valve is then opened, which allows the gas in the reference cell to expand into a connected chamber of known volume and pressure (V_1 and P_1, with $P_2 > P_1$) which contains the core sample of unknown grain volume. The equilibrium pressure P_e is then measured, and grain volume (V_g) is calculated from Boyle's Law expressed as

$$P_1(V_1 - V_g) + P_2V_2 = P_e(V_1 + V_2 - V_g) \qquad (1.1.3)$$

Re-arranging equation (1.1.3) yields

$$V_g = \frac{P_e V_1 + P_e V_2 - P_1 V_1 - P_2 V_2}{P_e - P_1} \quad (1.1.4)$$

Another approach is the 'absolute porosity method' in which the sample is disaggregated to grain size after measuring the dry weight and bulk volume, and the grain volume is determined using the immersed body method described above.

1.1.3.3 Pore Volume

Pore volume can be measured directly using a number of methods. In the 'wet and dry method', the pore-space is filled with liquid of known density, and the mass change is measured at constant temperature and pressure. The pore-volume is then calculated using

$$V_p = \frac{\Delta m}{\rho} \quad (1.1.5)$$

where Δm is the change in mass and ρ is the fluid density. The 'summation of fluids' method simply measures the total volume of fluid recovered from the sample during cleaning after recovery to surface (e.g. Dean Stark) to give a direct estimate of the pore-volume. However, pore volume is often calculated indirectly using the measured values of bulk and grain volume and equation (1.1.1).

1.1.4 Grain Density

Grain density is defined as

$$\rho_g = \frac{m_s}{V_g} \quad (1.1.6)$$

where m_s is the mass of the dry sample and V_g is the grain volume. The grain density is typically calculated by simply weighing a dry sample on a precise balance and dividing the measured weight by the grain volume measured using the Boyle's law method or calculated from measurements of the bulk volume and pore volume.

Laboratory measurement techniques of porosity have not changed significantly in the last few decades. Accuracy of the measurement may be affected by several factors such as grain volume measurement accuracy and grain losses in some cases. When comparing experimentally measured porosities with wireline-log derived values, effects of sample preparation and representativeness of sample volume should be taken into account.

1.2 Permeability

1.2.1. Darcy's Law

The ability of a porous rock to transmit fluid is quantified by the property called *permeability*. Quantitatively, permeability is defined by *Darcy's law*. This law was formulated by French civil engineer Henry Darcy in 1856 on the basis of his experiments on water filtration through sand beds. *Darcy's law is the most important equation in subsurface reservoir engineering, and other related fields such as groundwater hydrology*.

Imagine a fluid having viscosity μ, flowing through a horizontal tube of length L and cross-sectional area A, filled with a porous material such as rock or sand. The fluid pressure at the inlet is P_i, and at the outlet is P_o, as in Fig. 1.2.1. The rock and fluids are *incompressible* i.e. their volume does not change with changes in pressure.

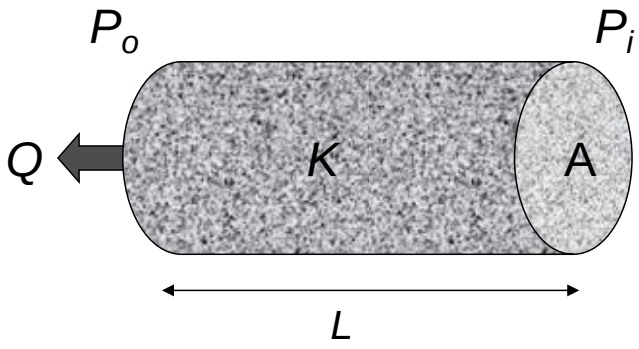

Fig. 1.2.1. Experimental set-up for measuring the permeability of a porous rock. The sample shown represents a typical cylindrical core plug of rock measuring c. 4-10cm in length and 1 – 3cm in diameter.

According to Darcy's law, the fluid will flow through the rock in the direction from higher pressure to lower pressure, and the volumetric flowrate of this fluid will be given by

$$Q = \frac{kA(P_i - P_o)}{\mu L} = \frac{kA}{\mu}\frac{\Delta P}{L} \qquad (1.2.1)$$

where: Q = volumetric flowrate, with units of [m^3/s]
k = *permeability* of the rock, with units of [m^2]
A = cross-sectional area of the rock core, with units of [m^2]
P_i , P_o = inlet/outlet pressures, with units of [Pa]
μ = viscosity of the fluid, with units of [Pa s]
L = length of the core, with units of [m]

This equation can be thought of as providing a definition of permeability, and it also shows us how to measure the permeability in the laboratory. It tells us that the flowrate is proportional to the area, inversely proportional to the fluid viscosity, and proportional to the pressure gradient, *i.e.*, the pressure drop per unit length, $\Delta P/L$. Note that the permeability is a *property of the rock*; the influence of the fluid that is flowing through the rock is represented by the viscosity term in Darcy's law.

It is usually more convenient to work with the volumetric flow per unit area, $q = Q/A$. Darcy's law is therefore usually written as

$$q = \frac{Q}{A} = \frac{k(P_i - P_o)}{\mu L} = \frac{k}{\mu}\frac{\Delta P}{L} \qquad (1.2.2)$$

where the flux q has dimensions of [m/s]. The flux q defined in this way is also sometimes termed the 'filtration velocity' or 'Darcy velocity' of the flow.

The flux q is not the same as the velocity of the fluid in the pore-space, because the particles flow only through the pores, but the flux is defined by the total cross-sectional area A that includes both pores and grains. Moreover, the velocity in the pore-space will be highly variable, depending upon the pore-size, pore-shape, and pore-connectivity. If the flux is defined instead by the cross-sectional area of the pores A_{pore}, then we have

$$q_{pore} = \frac{Q}{A_{pore}} = \frac{q}{\phi} \tag{1.2.3}$$

where $A_{pore} = A\phi$. The flux q_{pore} defined in this way is sometimes termed the 'intrinsic velocity' of the fluid, and it represents an average velocity of the fluid in the pore-space.

For the general case in which the flux may vary from point-to-point, we need a *differential* form of Darcy's law which is valid at a single point in space (the REV). The *differential* version of equation (1.2.2) for horizontal flow is

$$q_x = -\frac{k}{\mu}\frac{dP}{dx} \tag{1.2.4}$$

The minus sign is included because the fluid flows in the direction from *higher* to *lower* pressure. Note that equation (1.2.4) is valid for both compressible and incompressible fluids and rocks because it is defined at a single point in terms of the pressure *gradient*, not the pressure *difference* over a finite distance L.

For vertical flow, we must include a gravitational term in Darcy's law, to account for the hydrostatic pressure gradient found even within a stagnant fluid owing to the weight of the overlying fluid. Assuming the fluid density ρ is constant (i.e. the fluid is incompressible), the pressure at depth z below some (arbitrary) datum level is given by

$$P(z) = P_d + \rho g z \tag{1.2.5}$$

where P_d is the pressure at the datum.

Equation (1.2.5) shows there is a vertical pressure gradient in a stagnant fluid, but there is no flow. The hydrostatic (or equilibrium) pressure gradient is (from equation (1.2.5))

$$\left.\frac{dP}{dz}\right|_{hydrostatic} = \rho g \tag{1.2.6}$$

Fluid will flow vertically through the rock only if the imposed pressure gradient exceeds the hydrostatic pressure gradient given by (1.2.6), so the actual driving force should be $(dP/dz) - \rho g$. Equation (1.2.4) is therefore modified for vertical flow to yield

$$q_z = -\frac{k}{\mu}\left(\frac{dP}{dz} - \rho g\right) = -\frac{k}{\mu}\frac{d}{dz}\left(P - \rho g z\right) = -\frac{k}{\mu}\left(\frac{dP}{dz} - \frac{d}{dz}\left(\rho g z\right)\right) \tag{1.2.7}$$

Actually, this form of the equation also holds for horizontal flow, because there is no hydrostatic pressure gradient in the horizontal direction, so the last term on the right-hand-side $d(\rho g z)/dz = 0$. A convenient way of simplifying equation (1.2.7) is to define the fluid potential, which is the pressure above hydrostatic at a given location

$$\Phi(z) = P(z) - \rho g z \tag{1.2.8}$$

in which case equation (1.2.7) can be generalized to any flow direction n (where n denotes the x, y or z directions)

$$q_n = -\frac{k}{\mu}\frac{d\Phi}{dn} \tag{1.2.9}$$

The above equations assume that the permeability is the same in all directions. But in most reservoirs, the permeability in the horizontal plane (parallel to bedding), k_h, is different than the vertical permeability (perpendicular to bedding), k_v. Typically, $k_v < k_h$. The permeabilities in different directions within the horizontal plane may also differ, but this difference is usually not as great as between k_h and k_v. The property of having different permeabilities in different directions is known as *anisotropy* (e.g. Fig. 1.2.2).

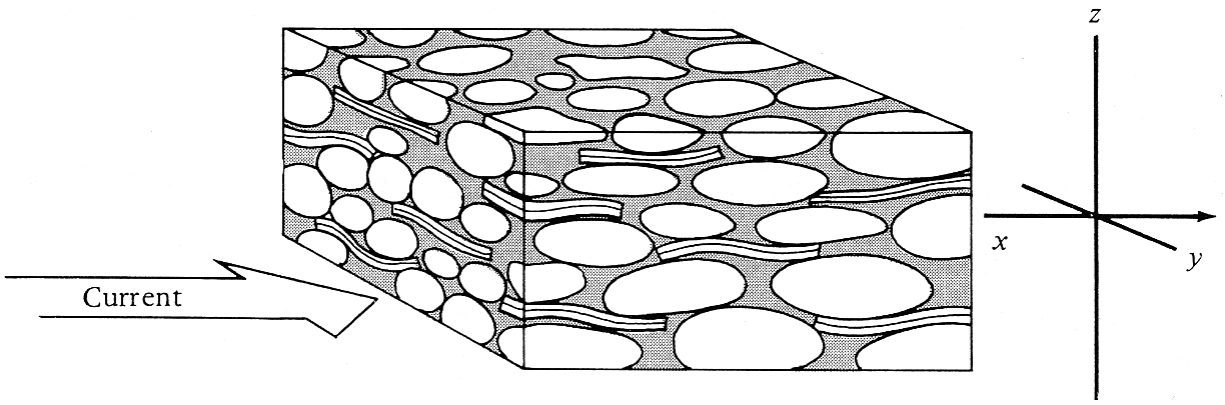

Figure 1.2.2. The permeability of a rock may be anisotropic at the scale of the REV because the grains (especially platy clay minerals) may have large aspect ratio and are generally oriented with the long axis parallel to the flow during deposition (shown here by the 'current'.)

For flow in an anisotropic rock, we must modify Darcy's law as follows:

$$q_h = -\frac{k_h}{\mu}\frac{d\Phi}{dx} \tag{1.2.10a}$$

$$q_v = -\frac{k_v}{\mu}\frac{d\Phi}{dz} \tag{1.2.10b}$$

If the rock is anisotropic, eq. (1.2.10) does not hold in an *arbitrary* direction, even if we use an appropriate value of k. The correct version of Darcy's law for an anisotropic rock must be written in terms of the *permeability tensor*, which is a symmetric 3x3 matrix that has *six* independent components k_{xx}, k_{yy}, k_{zz}, k_{xy}, k_{xz}, k_{yz}.

Darcy's Law is defined assuming laminar flow in the pore-space (i.e. for low Reynolds number) when inertial effects can be neglected. The Reynolds number can be written in this context as

$$\mathrm{Re} = \frac{2\rho q_{pore} R}{\mu} \tag{1.2.11}$$

The Reynolds number increases with increasing fluid velocity or decreasing fluid viscosity and, at sufficiently high Reynolds number, flow in the pore-space becomes turbulent. If this is the case, we must modify Darcy's law by incorporating a quadratic term in velocity q^2 on the left-hand side of, say, eq. (1.2.4).

$$\frac{dP}{dx} = -\frac{\mu}{k}q - \beta\rho q^2 \qquad (1.2.12)$$

where ρ is density and β is the '*Forcheimer correction factor*' (sometimes, $1/\beta$ is known as the 'inertial permeability'). The resulting more general equation (1.2.12), called the Forcheimer equation, is required in some situations, such as gas flow (gas has low viscosity) and near the wellbore (where the velocities are higher). However, Darcy's law is adequate in most situations.

1.2.2. Units of Permeability

Permeability has dimensions of area, so in the SI system it has units of [m^2]. However, in most areas of engineering it is conventional to use a unit called the 'Darcy', which is defined by

$$1 \text{ Darcy} = 0.987 \times 10^{-12} \text{ m}^2 \approx 10^{-12} \text{ m}^2 \qquad (1.2.13)$$

This unit is defined such that a rock having a permeability of 1 Darcy would transmit 1 cm^3 of water (which has a viscosity of 1 centiPoise, or 0.001 Pa s) per second through a region that has a cross-sectional area of 1 cm^2, if the pressure gradient along the direction of flow is 1 atm / cm. This definition is strange, in that it utilises different systems of units.

Some people apply Darcy's law by first converting flowrates to cm^3/s, converting areas to cm^2, viscosity to cP and pressures to atm, in which case the value of k must be expressed in Darcies. Another method is to first convert all parameters to SI units, in which case the value of k must be expressed in units of m^2. When making practical calculations of permeability, it is generally sensible to set up a spreadsheet or other automated method for making unit conversions, rather than implementing the conversions each time by hand for a given calculation.

Rock type	k (Darcies)	k (m^2)
Coarse gravel	$10^3 – 10^4$	$10^{-9} – 10^{-8}$
Sands, gravels	$1 – 10^4$	$10^{-12} – 10^{-9}$
Fine sand, silt	$10^{-4} – 1$	$10^{-16} – 10^{-12}$
Clay, mudstones	$10^{-9} – 10^{-6}$	$10^{-21} – 10^{-18}$
Limestone	$10^{-6} – 10$	$10^{-18} – 10^{-9}$
Sandstone	$10^{-5} – 10$	$10^{-17} – 10^{-11}$
Weathered chalk	$1 – 100$	$10^{-12} – 10^{-10}$
Unweathered chalk	$10^{-9} – 0.1$	$10^{-21} – 10^{-13}$
Granite, gneiss ('basement')	$10^{-8} – 10^{-4}$	$10^{-20} – 10^{-16}$

Table 1.2.1. Typical permeability ranges for a variety of sands and rock types.

Table 1.2.1 shows that the permeability of geological media varies over many orders of magnitude. However, most reservoir rocks have permeabilities in the range of 0.1 milliDarcies (mD) to 10 Darcies (D), and usually in the much narrower range of 10-1000 mD.

1.2.3. Relationship between Permeability and Pore Size

The permeability depends on the porosity of the rock, and also on the *pore size*. Many models have been developed to try to relate permeability to porosity, pore size, and other attributes of the pore space, and just one will be presented here to illustrate the key concepts. It can be shown (see derivation below) that if the rock is modelled as a simple bundle of parallel circular tubes of the same diameter d (Fig. 1.2.3) then the permeability is given by

$$k = \phi d^2 / 96 \qquad (1.2.14)$$

This equation is often written in terms of the specific surface S/V, the total amount of pore surface area S per unit volume of rock V; the result is

$$k = \phi^3 / \left(6(S/V)^2\right) \qquad (1.2.15)$$

This is often called the *Kozeny-Carman* equation. One justification for this equation is that the permeability is the inverse of the 'hydraulic resistivity' and it is plausible that the resistance to flow, which is essentially due to viscous drag of the fluid against the pore walls, is related to the surface area of the pores. In some versions of the Kozeny-Carman equation, the factor 6 is replaced by another constant called the 'tortuosity', τ. The tortuosity is sometimes (and probably erroneously) claimed to represent the ratio of the actual fluid flow path from inlet to outlet, to the nominal fluid flow path L, but it is preferable to think of it as nothing more than an empirical fitting factor.

There have been many attempts to try to improve upon the Kozeny-Carman equation, by incorporating more information about the distribution of pore sizes, interconnectedness of the pores, *etc*. For our present purposes, it is sufficient to understand that the permeability is proportional to the square of the mean pore diameter. This is why grain size (which is closely related to pore-size) plays such a key role in controlling permeability.

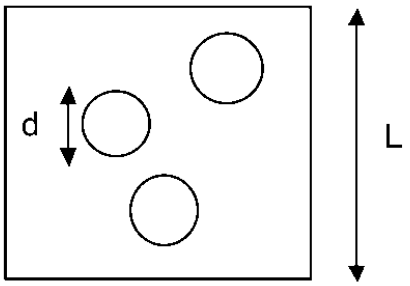

Fig. 1.2.3. Idealised pore structure used to derive a relationship between permeability, porosity and pore size.

1.2.4 Measurement of Permeability

The most direct way of measuring permeability is to conduct flow experiments using cores of different types. Well test analysis also gives information on permeability at a larger volume scale, if the test is designed properly and the interpretation model is well constrained by geological and geophysical data. An important point here is that permeability is defined by an equation for flow; hence the only methods that allow proper determination of permeability induce flow, either in rock samples at the surface, or rock in the reservoir. Moreover, because rocks are inherently heterogeneous and because permeability strongly varies with pore/grain size, measured values of permeability are strongly scale-dependant.

1.2.4.1 Steady-State Measurement

A geometrically regular core sample of known length and diameter is placed into a Hassler-type core holder (Fig. 1.2.4), and a fluid (typically gas or brine) is caused to flow through the sample. A Hassler core holder is widely used in coreflooding experiments: it is a strong sleeve (constructed from steel or Hastelloy) within which the core sample is placed. End caps are then attached to the sleeve to hold the sample in place, and a confining pressure is applied that tightly seals the sample within the sleeve. The confining pressure ensures that there is no leakage around the side of the

sample; fluids are forced to pass in or out only through the opposing ends of the sample. The end caps have flowlines that pass through them allowing fluids to enter and leave the sample.

*Derivation 1: The Kozeny-Carman equation for permeability using a capillary tubes model (***THESE DERIVATIONS ARE OPTIONAL – FOR THE INTERESTED STUDENT ONLY***)*

The simplest model of a rock assumes that the pores are all circular, parallel tubes of the same diameter. Consider a set of circular pore tubes, each of diameter d, passing through a cubical rock specimen of side L, as in Fig. 1.2.3, with a pressure difference ΔP imposed across the two parallel faces (on the page and behind the page) of the rock.

According to Poiseuille's equation for pipe flow, the flow through each tube is given by

$$Q = -\frac{\pi d^4}{128\mu}\frac{\Delta P}{L} \tag{1.2.16}$$

If there are N such pores, the total flow rate will be

$$Q = -\frac{\pi N d^4}{128\mu}\frac{\Delta P}{L} \tag{1.2.17}$$

The total area of these pores, in the plane of the page, is $A_{pore} = N\pi d^2/4$, and the porosity is $\phi = A_{pore} / A = A_{pore} / L^2$, so the total flowrate is

$$Q = -\frac{\phi A d^2}{32\mu}\frac{\Delta P}{L} \tag{1.2.18}$$

If we compare this flowrate with Darcy's law (e.g. equation 1.2.1) we see that the permeability of this rock is $k = \phi d^2/32$. Lastly, we note that an isotropic rock should have only one-third of its pores aligned in each of the x, y and z directions, so the permeability of this idealised porous rock in a given direction is given by equation (1.2.14).

A slightly more realistic model, in which the orientations of the pores are randomly distributed in three-dimensional space, leads to exactly the same result.

In brine permeability measurements, a pump is typically used to force the brine through the sample; in gas permeability measurements, the gas at the inlet side is at higher pressure than the outlet (high pressure laboratory line or bottle supply) and a valve is opened to allow the gas to flow through the sample. The core holder tightly confines the sample and ensures there is no flow of fluid around, rather than through, the sample. The flow rate Q through the sample is measured (or may be specified by the pump setting), as is the pressure drop $(P_i - P_o)$ across the sample, and the cross-sectional area A and length of the sample L. The viscosity of the fluid μ is known (or measured in a separate experiment), and Darcy's Law is then used to calculate the sample permeability. For brine, which is close to incompressible, the expression is

$$Q_{brine} = \frac{k_{brine} A\left(P_i - P_o\right)}{\mu_{brine} L} \tag{1.2.19}$$

so the permeability to brine is given by

$$k_{brine} = \frac{Q_{brine}\mu_{brine}L}{A(P_i - P_o)} \tag{1.2.20}$$

(cf. equation 1.2.2).

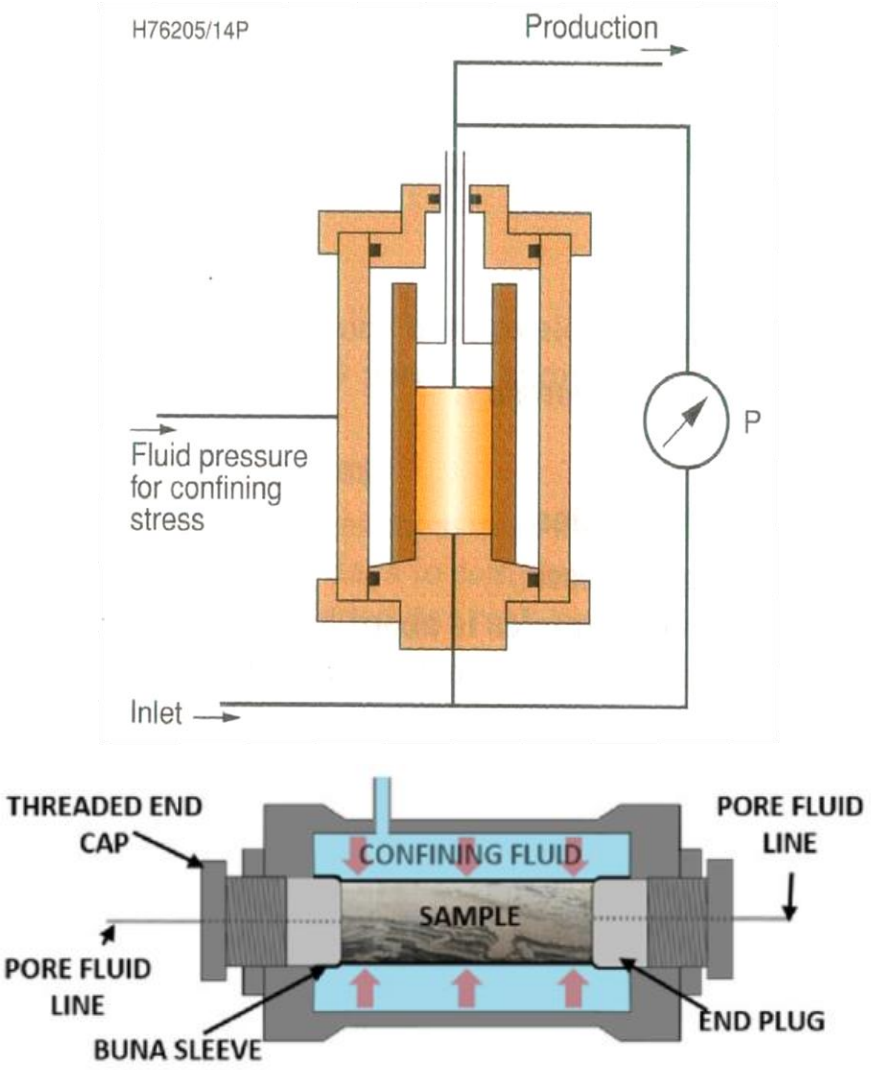

Figure 1.2.4. Schematic of a Hassler cell used here to measure permeability. The pressure transducer measures the pressure drop along the plug, and the flow rate is measured. Upper figure shows the overall setup; lower figure shows the Hassler cell in which the sample is held.

However, for gas, which is typically air or nitrogen, Darcy's law applied along the length of the plug must be modified to account for the compressibility of the gas and the pressure difference at the inlet and outlet, yielding

$$k_{gas} = \frac{2Q_{gas}\mu_{gas}LP_{ref}}{A(P_i^2 - P_o^2)} \tag{1.2.21}$$

where P_{ref} is the pressure at which the flow rate is measured. Note that the differential form of Darcy's Law, expressed in terms of the pressure *gradient* and applied to an infinitesimally small REV which is treated mathematically as a single point in space (e.g. equation 1.2.4), is valid regardless of the compressibility of the fluid; we only need to account for compressibility here

because Darcy's Law is applied to a finite volume of rock of length *L*, across which there is pressure *difference*. Note also that pressure in equation (1.2.21) is *absolute* (relative to a vacuum) rather than *gauge* (relative to atmospheric pressure).

For detailed analysis of spatial permeability variation in the core, a probe permeameter (minipermeameter) can be used. A schematic of a probe permeameter is shown in Figure 1.2.5. In the probe permeameter, gas flows from the end of a small-diameter probe that is sealed against the surface of a slabbed or exposed core. The gas flow rate and the pressure in the probe are measured and used for permeability calculation. As the measured permeability is localized to a small region near the seal, this technique is particularly useful for characterizing small-scale geological heterogeneities. Typically, the probe permeability measurement results in a permeability profile along the core, or a 2-dimensional array across a slabbed core face. The data obtained data can be calibrated against the core plug permeability measurements (e.g. Fig. 1.2.6), or used to populate 'mini-models' of the heterogeneity of interest.

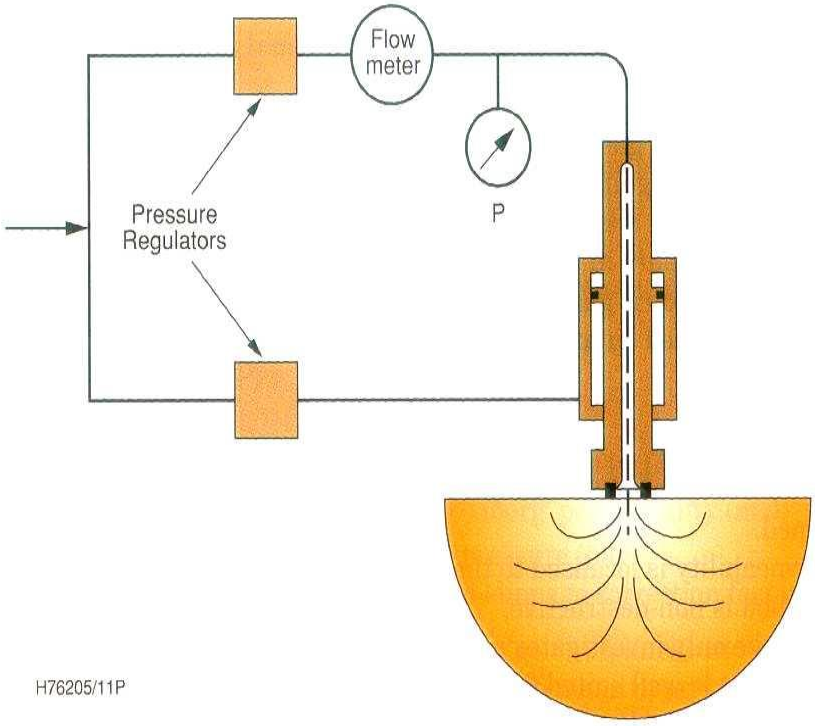

Figure 1.2.5 Schematic of a probe permeameter (mini-permeameter). The tip is typically a few mm in diameter.

1.2.4.2 Unsteady-State Measurement

Increases in computational power along with improved accuracy of pressure transducers, along with increasing interest in very low permeability rocks (for example, as CO_2 seals) have led to increased popularity of unsteady-state permeability measurements. Figure 1.2.7 illustrates a *pulse decay permeameter*. A dry sample is placed into the core holder, and a pressure pulse is introduced by transiently increasing the pressure in the upstream vessel. The system is then allowed to return to the equilibrium pressure, and the rate at which equilibrium is approached depends upon the permeability of the core sample. However, it is not necessary to wait until the equilibrium is reached. Therefore, this technique (or one of its variations) is particularly useful for low permeability samples (below 0.1mD) where steady-state measurements may take a prohibitively long time to reach pressure/flow equilibrium.

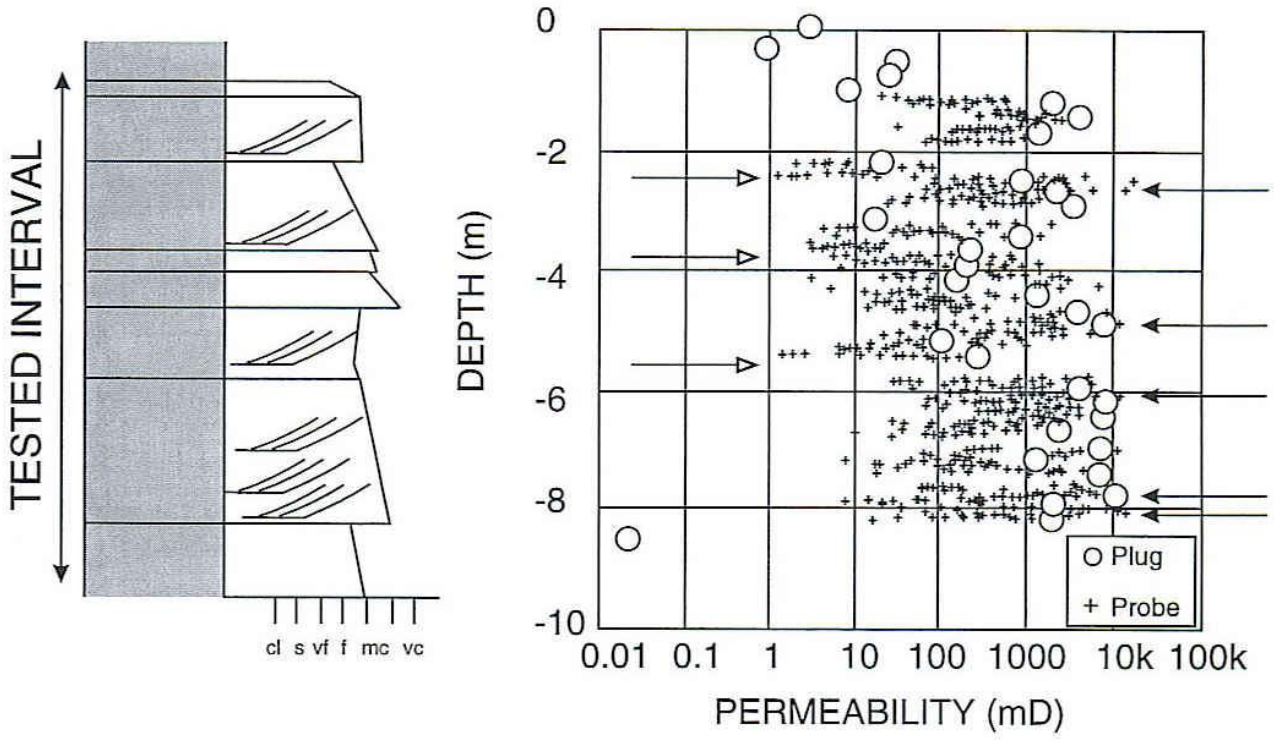

Figure 1.2.6 Comparison of plug and probe permeameter measurements.

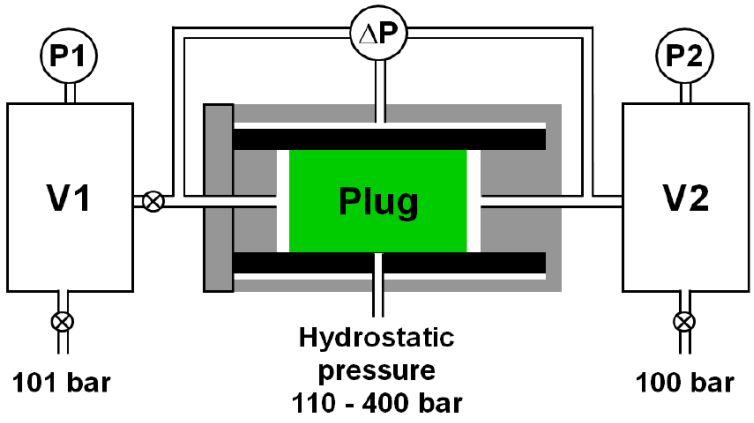

Figure 1.2.7. Schematic of a pulse decay permeameter.

1.2.4.3 Whole Core Measurement

Whole core measurements are used to obtain permeability data at a scale larger than that of a core-plug. The whole core is prepared in the same manner as the plugs. It is then placed into a rubber sleeve of a (large) core holder. The diameter of the core is of order 5-8 cm, and the length is typically of order 1-2m. A schematic of a whole core measurement apparatus is shown in Figure 1.2.8. The principle is the same as the steady-state measurements. Vertical permeability can easily be determined by flowing (typically) gas through the length of the core. However, horizontal permeability measurement is more complex. Gas is flowed into cylindrical surface of the sample using an array of permeable screens, which cover opposing quadrants of the surface, and are rotated through 90º so that measurements can be carried out in two perpendicular orientations. The higher of the two horizontal permeabilities is referred to as k_{max} and the lower as k_{90}. A geometric mean permeability is calculated to represent k_h, which is used in porosity-permeability correlations and in log calibration for permeability estimation.

1.2.5 Factors Affecting Permeability Measurement

The permeability of a core sample can be affected by a variety of phenomena. Gas slippage, confining pressure, pore content, inertial (turbulence) effects and improper plug cleaning/drying are a few examples. Therefore, certain precautions should be taken while preparing the sample and conducting the measurement.

1.2.5.1. Gas Slippage. Klinkenberg reported variations in measured permeability when comparing data obtained using non-reactive liquids versus gases. These variations are associated with an effect called gas slippage, which can be described as the ability of a gas molecule to more easily retain forward velocity along a solid interface compared to a liquid molecule. Liquid velocities normally approach zero at the solid wall. However, gas molecules have a nonzero wall velocity (e.g. Fig. 1.2.9). This may result in two different measurements of rock permeability depending on the fluid used in the experiment. Since permeability is an intrinsic property of the rock, it should be independent of the fluid properties. Therefore, data obtained through gas injection should be corrected.

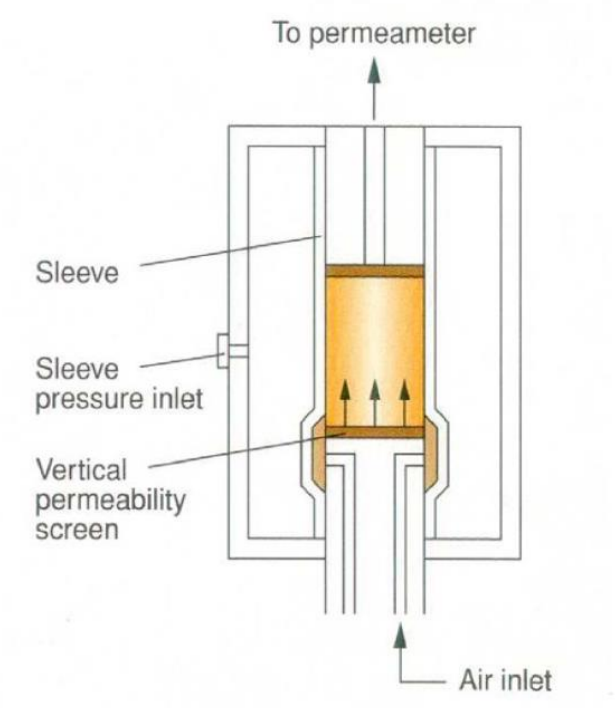

Figure 1.2.8. Schematic of whole core permeability measurement apparatus.

Klinkenberg showed that measured permeability values are higher at low mean (average) pressures when gas molecules do not adhere to the pore walls as liquid molecules do. This so-called slippage effect decreases with increasing pressure, as gas begins to act like a liquid once the flowing pressure increases. Experimental data show that a plot of reciprocal of mean flowing pressure with respect to permeability yields a straight line. The straight line can be extrapolated to infinite mean pressure and the permeability value at the extrapolated point is referred as the equivalent liquid permeability. A graphical illustration is shown in Figure 1.2.10. The mathematical expression of this phenomenon is called the Klinkenberg equation and can be written as:

$$k_l = \frac{k_g}{\left(1+\frac{b}{P_m}\right)} \qquad (1.2.22)$$

where k_l is the equivalent liquid permeability, k_g is the measured gas permeability at the mean flowing gas pressure P_m, and b is the 'Klinkenberg constant' which is a fitting parameter dependent on the type of rock and the gas used in the experiment. Note that the correction factor, on a percentage basis, is greater for low permeability rocks and low-pressure conditions. It becomes smaller as the permeability and/or the pressure increase. It is usually negligible at reservoir conditions due to the large fluid pressure; thus, gas slippage is a phenomenon of relevance only to laboratory experiments.

1.2.5.2. Confining Pressure. Ideally, permeability (and porosity) measurements should be obtained with a net overburden pressure in order to simulate the reservoir conditions. It has been found that overburden pressure reduces the measured permeability values (Fig. 1.2.11). The impact is observed more on unconsolidated rocks and on samples containing fractures and microcracks. In order to better understand and account for its impact, a series of confining stress measurements should be performed on selected samples.

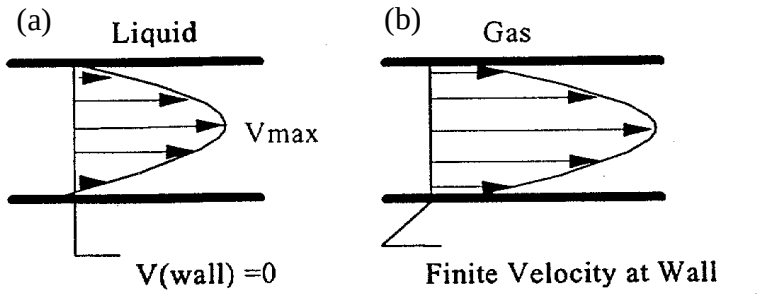

Figure 1.2.9. Velocity profile for a liquid (a) and gas (b) flowing through a simple pore, showing the 'slippage' (non-zero velocity) at the pore wall when gas is flowing at low pressure.

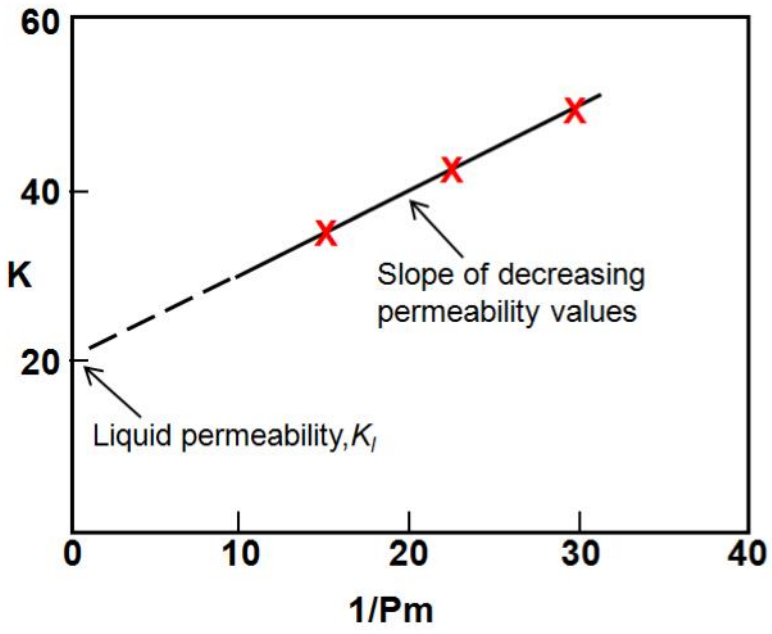

Figure 1.2.10 Illustration of the Klinkenberg permeability correction. The crosses are the measured permeability values at different pressures. From equation 1.2.22, the straight line has gradient $k_l b$ and is extrapolated to infinite mean pressure ($1/p_m = 0$). The permeability value at the intercept is the equivalent liquid permeability k_l.

1.2.5.3. Inertial Effects. If the gas flow rate through the core is high, inertial effects may become important and should be accounted for. They usually generate an additional pressure drop compared to laminar flow and may result in underestimation of permeability if not properly accounted for.

Although it is often evident in laboratory studies, turbulence effects are in general only applicable in the near wellbore region of high-rate gas flow. High-production gas wells have demonstrated the need for extended core analysis that provides a non-Darcy flow coefficient. The Forcheimer correction factor, β, is commonly reported along with the gas permeability measurements in these kinds of specific circumstances. The general form of the Forcheimer equation is given by equation (1.2.12).

1.2.5.4. Reactive Liquids. Although water is often considered to be a non-reactive fluid, it commonly interacts with clay minerals in a manner that impacts on permeability measurements, through hydration of the clay minerals and expansion of the clay layers in a process commonly termed 'clay swelling'. The effect of clay swelling is greater when the brine salinity is low (i.e. water is 'fresh'). Therefore, extra care should be taken while choosing the proper core plugging, cleaning and drying techniques for clay-bearing samples. For example, fresh water should be avoided while drilling a plug from the core; rather, brine with an appropriate salinity level and ion-balance should be used.

Permeability reduction may also be encountered due to particle movement (so-called 'fines migration') which is a function of flow velocity and fluid density. It may be necessary to determine a maximum displacement rate for experimental studies that avoids the initiation of fine particle migration.

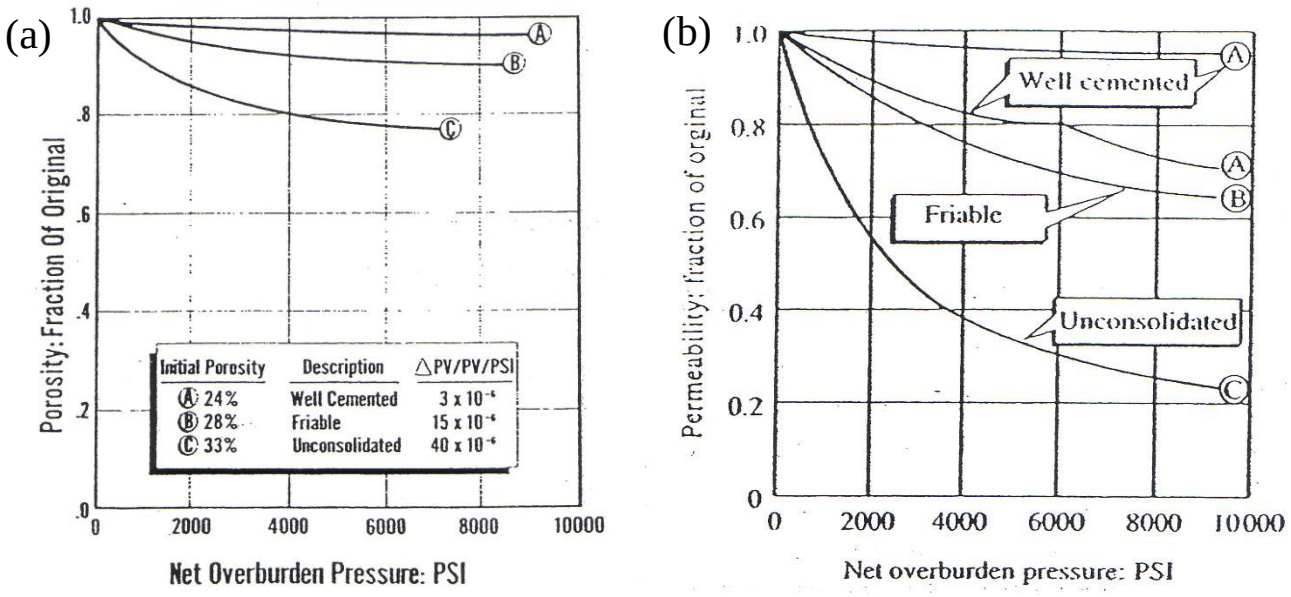

Figure 1.2.11 Effect of overburden on measured porosity (a) and permeability (b).

2. Definition and measurement of electrical properties

2.1. Electrical Conductivity

2.1.1. Definition of electrical conductivity and resistivity

The electrical conductivity of a rock is not a property that directly affects fluid flow; nor does it appear in the governing equations of fluid flow in a reservoir. But it is nevertheless very important in reservoir engineering, because it can be measured *in situ* using *logging tools*, and its value can then be used to infer the fluid saturation.

The flow of electrical current is governed by *Ohm's law*, which states that the current, *I*, flowing through any conductor, is equal to the voltage drop, *V*, divided by the resistance, *R*

$$I = \frac{V}{R} \tag{2.1.1}$$

Electrical charge has units of Coulombs, so current, which is the flow of charge, has units of Coulombs/second. Resistance therefore has units of volt-seconds/Coulomb, which are also known as *Ohms*. In this form, *R* depends on the material properties and also on the shape and size of the conductor.

Now consider a cylindrically-shaped conductor, of length *L* and cross-sectional area *A*, as in figure 2.1.1. All other factors being equal, the current will be proportional to *A*, and inversely proportional to *L*. So, we expect that the resistance can be expressed as

$$R = \rho \frac{L}{A} \tag{2.1.2}$$

where ρ is the *resistivity*, which is an intrinsic property of the material, and does not depend on the geometry of the conductor. The resistivity has units of Ohm-meters (Ωm).

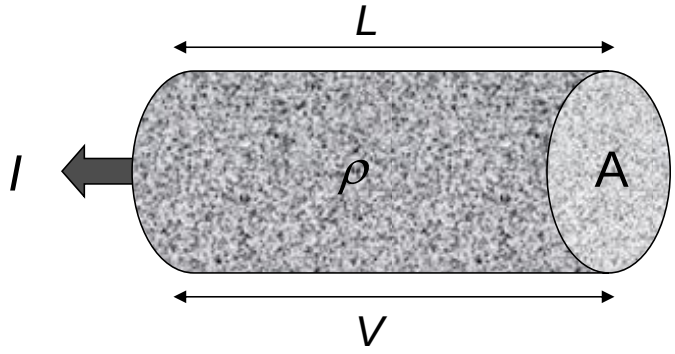

Figure 2.1.1. Electrical current through a cylindrical conductor of length L, area A and resistivity ρ.

Hence, eq. (2.1.1) can be written as

$$I = \frac{A}{\rho}\frac{V}{L} \tag{2.1.3}$$

We can also define the conductivity as $\sigma = 1/\rho$, in which case we can write (2.1.3) as

$$I = \sigma A \frac{V}{L} \tag{2.1.4}$$

In this form, it is clear that Ohm's law is mathematically analogous to Darcy's law, with current I (the flow of electrical charge) being analogous to fluid flux Q, voltage drop V analogous to pressure drop ΔP, and electrical conductivity σ analogous to the ratio of permeability/viscosity k/μ (*i.e.*, the mobility) (compare with equation 1.2.1). The electrical conductivities of the minerals that typically form reservoir rocks are very low. But the water that partially or completely fills the pore space of reservoir rocks always contains salts such as NaCl or KCl, which render the water conductive. The conductivities of these "*brines*" are typically ten orders of magnitude higher than that of the rock minerals. Hence, electrical current in a reservoir rock will flow mainly through the portion of the pore space that is occupied by brine, and the total conductivity of the brine saturated rock will be some function of the brine conductivity, and some function of the rock.

2.1.2. Archie's First Law

We are not particularly interested in the brine conductivity, so it would be preferable to identify a parameter that reflects only the properties of the rock. We do this by defining (in general, independent of any pore geometry model) the *formation resistivity factor*, also known as the *formation factor*, which is the ratio of the conductivity of the brine (σ_w) to the effective conductivity of the brine-saturated rock (σ_{rs}):

$$F = \frac{\sigma_w}{\sigma_{rs}} \tag{2.1.5}$$

The resistivity is the inverse of the conductivity, so we can also say that

$$F = \frac{\rho_{rs}}{\rho_w} \tag{2.1.6}$$

It can be shown (see Derivation 2) that, for a bundle of capillary tubes model, F is given by

$$F = \frac{\sigma_w}{\sigma_{rs}} = 3\phi^{-1} \tag{2.1.7}$$

Note that in contrast to the permeability, which has a strong dependence on pore size, the formation factor, according to the bundle of tubes model, has no dependence on pore size but it does depend on porosity.

This capillary-tube model correctly tells us that F will be larger for less porous rocks, but otherwise it is not accurate enough for engineering purposes. Experimental measurements of F tend to show a stronger dependence on porosity than the –1 power that appears in eq. (2.1.7). Archie (1942) proposed generalising eq. (2.1.7) by replacing the factor of 3, and the exponent –1, with parameters that may vary from rock to rock. The result is the "Archie's law":

$$F = a\phi^{-m} \tag{2.1.8}$$

The parameter a is often called the *tortuosity*, and m is called the *cementation index*, but these names are outdated and not very useful; it is preferable to think of them as simple empirical fitting parameters to experimental data.

Archie's law in the form of (2.1.8) can fit many sets of data from different rocks from the same reservoir. For sandstones, the exponent *m* usually lies between 1.5 and 2.5, and is often close to 2 (e.g. Table 2.1.1). The parameter *a* is usually close to 1.0. Figure 2.2.2 shows some data on Vosges and Fontainebleau sandstones fitted with $a = 0.496$, and $m = 2.05$.

Sediment type	*m*	Comments
Sandstone		
Unconsolidated	1.4-1.5	*m* largely correlates
Very slightly cemented	1.5-1.7	with cementation
Moderately cemented	1.8-1.9	
Highly cemented	2.0-2.2	
Limestone		
Chalk	1.7-1.8	*m* largely correlates
Crystalline and granular	1.8-2.0	with porosity type
Vuggy carbonate	2.1-2.6	

Table 2.1.1. Typical values of m for various rock types.

Although Archie's "law" is extremely useful in petrophysics, it should nevertheless be remembered that it is not a fundamental law of rock physics but is merely a convenient curve-fit that is usually sufficiently accurate for engineering purposes. It might appear that we could use Archie's law to estimate porosity, but there are much more accurate ways to estimate ϕ both in the laboratory and using wireline tools. The usefulness of Archie's law, and of resistivity measurements in general, is in estimating water saturation.

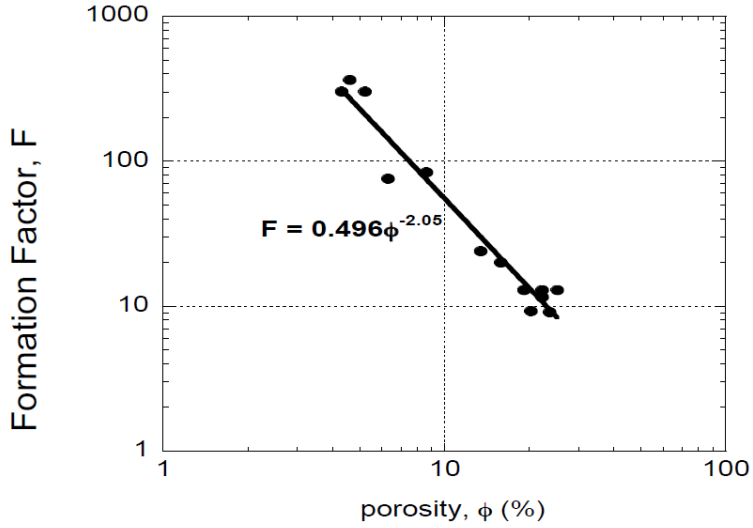

Figure 2.1.2. Example fit to data on Vosges and Fontainebleau sandstones, from Ruffet et al. (1991) with a = 0.496 and m = 2.05.

2.1.3. Archie's Second Law

For rocks that contain water and a second (non-conductive) fluid such as gas or CO_2, we use the following generalisation of Archie's law, which is sometimes called *Archie's second law*:

$$I = \frac{\rho_r(S_w)}{\rho_r(S_w = 1)} = \frac{\rho_{rw}}{\rho_{rs}} = \frac{\sigma_{rs}}{\sigma_{rw}} = S_w^{-n} \qquad (2.1.9)$$

where the rock conductivity when fully saturated with brine is denoted (σ_{rs}) and the conductivity at partial saturation is denoted (σ_{rw}), and n is called the *saturation exponent*. The parameter I is termed the 'resistivity index' and is given by the ratio of the resistivity of the rock at some saturation S_w to the resistivity of the rock when it is fully saturated with brine. Note that F and I are both positive numbers that are greater than 1.

Derivation 2: Archie's Law for a capillary tubes model

As with permeability and capillary pressure, we can get some idea of how the electrical conductivity depends on pore structure by appealing to the bundle of parallel tubes model. Consider such an idealised rock (Fig. 2.1.3), where A is the total area of the core, and the A_n are the areas of the individual pores.

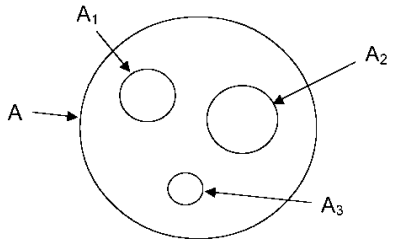

Figure 2.1.3. Bundle of capillary tubes model to calculate current through the saturated pore-space of a porous medium

Imagine that the pores are all filled with a brine of conductivity σ_w. If the core has length L into the page, and the rock is subjected to a voltage drop V along its length, then the current through the n-th tube will be

$$I_n = \sigma_w A_n \frac{V}{L} \tag{2.1.10}$$

The total current is the sum of the currents through each tube:

$$I = \sum_{n=1}^{N} I_n = \sum_{n=1}^{N} \sigma_w A_n \frac{V}{L} = \sigma_w \frac{V}{L} \sum_{n=1}^{N} A_n = \sigma_w \frac{V}{L} A_{pores} = \sigma_w \frac{V}{L} \phi A \tag{2.1.11}$$

If we compare this with Ohm's law, eq. (1.7.4), we see that the effective conductivity of the brine-saturated capillary tubes model is $\sigma_{eff} = \sigma_w \phi$, which means that the formation factor F (from equation 3.4.5) is given by

$$F = \frac{\sigma_w}{\sigma_{rs}} = \frac{1}{\phi} = \phi^{-1} \tag{2.1.12}$$

If we make the same argument as we did in the case of permeability that is only one-third of the capillaries are aligned in the direction of the voltage drop then we obtain equation (2.1.7). Archie's Law therefore applies to a rock comprising capillary tubes of random orientation if $a = 3$ and $m = 1$.

For rocks that contain water and a second, non-conductive fluid, we use the following generalisation of Archie's law, which is sometimes called *Archie's second law*:

$$I = \frac{\rho_r(S_w)}{\rho_r(S_w = 1)} = \frac{\rho_{rw}}{\rho_{rs}} = \frac{\sigma_{rs}}{\sigma_{rw}} = S_w^{-n} \qquad (2.1.13)$$

where the rock conductivity when fully saturated with brine is denoted (σ_{rs}) and the conductivity at partial saturation is denoted (σ_{rw}), and n is called the *saturation exponent*. The parameter I is termed the 'resistivity index' and is given by the ratio of the resistivity of the rock at some saturation S_w to the resistivity of the rock when it is fully saturated with brine. Note that F and I are both positive numbers that are greater than 1.

2.1.4 Surface electrical conductivity

If one assumes that n is constant throughout a reservoir, or at least throughout a certain rock unit, then eq. (2.1.13) implies that electrical resistivity measurements in a borehole can yield estimates of the water saturation. The situation is more complicated in shaly sands. In these rocks, the sand grains are coated by clay platelets which have a large negative surface electrical charge. An electrical double-layer develops along the surface of these plates, in which positive salt ions in the brine (such as Na^+) are attracted towards the mineral surface, leading to a local excess of electrical charge in the brine. This surface layer of excess charge allows another path for current, distinct from the current through the brine-saturated pores discussed above. To a good approximation, this surface current can be thought of as being in parallel with the pore current, and so it adds an extra component to the conductivity of the rock which is typically termed '*surface conductivity*'. This surface conductivity depends on the electrochemical properties of the clays, but not on the intrinsic conductivity of the brine; its *relative* contribution to the overall conductivity of the rock decreases as the brine conductivity increases. The resulting generalisation of Archie's Law for shaly sands is

$$\sigma_{rs} = \frac{1}{F}(\sigma_w + BQ_v) \qquad (2.1.14)$$

where Q_v is the charge on the double-layer, per unit volume, and B is a constant. Equation (3.4.14) is called the Waxman-Smits equation and is one of a number of approaches that attempt to account for the surface electrical conductivity of clay minerals.

Sediment type	*n*	Comments
Sandstone		
	1.42-2.55	Wyllie and Spangler, 1952
	1.12-2.52	Pierce and Loewe, 1958
	1.69-2.08	Walther, 1968
	1.65-2.38	Wilson and Hensel, 1982
	1.42-2.38	Hunt et al., 1985
Limestone		
	2.3-2.38	Walther, 1968
	1.1-1.9	Sharma et al., 1980
	1.65-2.22	Swanson, 1980

Table 2.1.*2. Typical values of n for various water-wet rock types.*

2.2 Measuring electrical properties

Measurements of electrical properties typically focus on determining the so-called Archie parameters (a, m, n) and any additional parameters required to relate electrical conductivity to water saturation (e.g. the cation-exchange-capacity Q_v or CEC).

2.2.1 Measuring formation factor

To determine *a* and *m*, the usual approach is to plot the formation factor *F* against the porosity ϕ for a number of plugs, on a log-log plot (or to plot log(*F*) versus log(ϕ) on a linear plot); recall that $F = \sigma_w/\sigma_{rs}$ by definition, where σ_w is the conductivity of the brine and σ_{rs} is the conductivity of the brine-saturated rock (equation 2.1.5), and that Archie's Law has $F = a\phi^{-m}$ (equation 2.1.8). Plotted in this way, a best-fit straight line through the data has the negative gradient *m*, and the *y*-axis intercept when $\phi = 1$ corresponds to *a* (e.g. Fig. 2.2.1). Values of *m* typically range from 1.5 - 2.5, and are often close to 2 (e.g. Table 2.1.1), whilst values of *a* range from 0.62 – 3.7. It is often argued that *a* should always be equal to 1, as any other value yields the rather nonsensical result that the electrical conductivity of the brine saturated plug when $\phi = 1$ (i.e. the rock is entirely void space) does not equal the electrical conductivity of the brine occupying the pore space! In reality, the measured values of *F* and ϕ rarely approach 1 (see, for example, Fig. 2.2.1), and using values of $a \neq 1$ to match the part of the parameter space where ϕ is small and *F* is large probably reflects the fact that there is not a genuinely linear relationship between *F* and ϕ^{-m} i.e. that Archie's 'Law' is not strictly valid. The point is that the chosen values of *a* and *m* should reflect the best match to the data over the range of values of *F* and ϕ relevant to the reservoir or rock unit of interest.

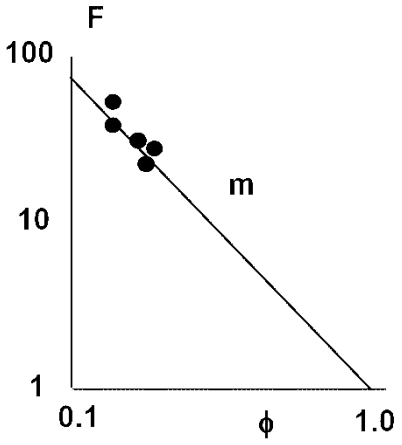

Figure 2.2.1. Estimation of the so-called 'cementation exponent' (m). The value is given by the negative gradient of a straight-line fit to measured values of formation factor (F) vs. porosity (ϕ) for a number of core samples from a given rock type, plotted on a log-log axis. The intercept with the y-axis when $\phi = 1$ yields the value of a. Here a = 1. See also Figure 1.7.3.

2.2.2 Measuring resistivity index

To determine *n*, the usual approach is to plot the resistivity index *I* against the water saturation S_w on a log-log plot (or to plot log(*I*) versus log(S_w) on a linear plot). From Archie's second law (equation 2.1.13), the resistivity index corresponds to

$$I = s_w^{-n} \qquad (2.2.1)$$

Plotted in this way, a best-fit straight line through the data has the negative gradient *n* (e.g. Fig. 2.2.2).

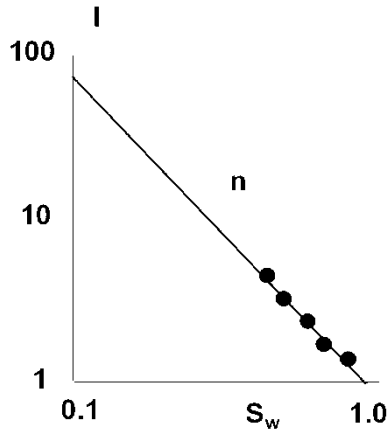

Figure 2.2.2. Estimation of the so-called 'saturation exponent' (n). The value is given by the gradient of a straight-line fit to measured values of resistivity index (I) vs. water saturation (S_w) for a particular core sample, plotted on a log-log axis.

To determine values of F requires measurements of the electrical conductivity of plugs of varying porosity; to determine values of I requires measurements of the electrical conductivity of one or more plugs for varying values of S_w. Electrical conductivity is typically measured using an LCR meter (inductance, capacitance, resistance meter) applying a potential difference across the plug that alternates at some frequency and measuring L, C and R over a range of frequencies, typically 10 Hz to 2 MHz. This approach is used to reduce electrode polarization effects, where the electrodes act like a capacitor, with charge accumulating at each electrode.

2.2.3 Measuring cation exchange capacity

A number of methods are available for measuring Q_v. The conductometric titration method, membrane potential method, and multiple salinity measurements, are a few examples. In the conductometric titration method, a clean sample is crushed and weighed. The exchangeable cations are exchanged using a suitable leaching solution and are quantified by conductometric titration, which involves titrating the solution whilst monitoring the conductivity, which displays a rapid increase after the correct titration has been reached. The conductometric titration technique is also known as the wet-chemistry method. It may not be recommended for an accurate Q_v measurement as the test is destructive. It involves crushing the sample, hence destroying the clay morphology and distribution, and creating additional ion exchange sites.

In the membrane potential measurement method, an electrical potential is generated when two brines of different salinity are brought into contact. The measured electrical potential increases when a shaly sample is positioned at the interface between the brines. The magnitude of the increase is directly related to Q_v. This technique is applicable for both consolidated and unconsolidated rocks. It is a non-destructive measurement, which properly incorporates the effects of clay distribution within the sample but may suffer from salinity-dependent electrode effects.

In a multiple salinity measurement, the conductivity of a brine-saturated rock sample, σ_{rw}, is measured at different brine salinities of known brine conductivity, σ_w. Four brines are usually used, starting with the lowest salinity. The sample is flooded with brine until the conductivity reaches equilibrium for different salinities. The quantity BQ_v, which is sometimes termed the 'clay conductivity' in the Waxman-Smits equation (2.1.14), is determined from the plot of σ_{rw} versus σ_w (see Figure 2.2.3). The 'clay corrected formation factor', F^*, is determined by fitting a straight line of slope $1/F^*$ through the high salinity data. Intrinsic Archie exponents m^* and n^* can be

determined through correlations of F^* with porosity. The clay conductivity, BQ_v, is obtained from the difference between $F^*\sigma_{rw}$ and σ_w.

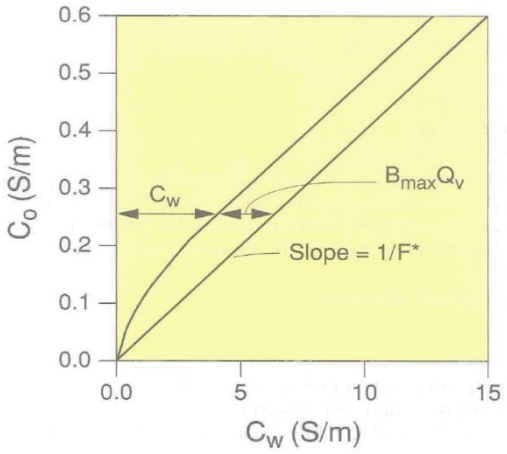

Figure 2.2.3. An illustration of brine saturated rock conductivity (C_o) vs. brine conductivity (C_w) plot for a shaly sandstone.

The equivalent conductance of clay-exchange cations, B, which is used to scale the cation exchange capacity per unit volume, Q_v, to units of conductivity, can be calculated as a function of brine conductivity, σ_w, and temperature, T (ºC). Although several different correlations have been suggested, the one developed by Juhasz is the most widely used:

$$B = \frac{-1.28 + 0.225T - 0.0004059T^2}{1 + \sigma_w^{-1.23}\left(0.045T - 0.27\right)} \qquad (2.2.2)$$

3. Definition and measurement of thermal properties

3.1. Thermal Conductivity

The thermal conductivity of a rock is very important in geothermal reservoirs and in thermal energy storage projects because it dictates the rate of heat transport by thermal conduction. Unlike permeability, reservoir thermal conductivity is a function of both the rock thermal conductivity and the thermal conductivity of the fluid(s) saturating the pore space.

The conduction of heat is governed by *Fourier's law*. Consider a cylindrically-shaped rock sample of length L and cross-sectional area A, as in Figure 1.2.1. The temperature at one end is T_i, and at the other end is T_o, as in Fig. 3.1.1, with $T_i > T_o$. According to Fourier's law, heat will flow through the rock in the direction from higher temperature to lower temperature, and the flow of heat will be given by

$$Q_h = \frac{k_t A(T_i - T_o)}{L} = k_t A \frac{\Delta T}{L} \qquad (3.1.1)$$

where: Q_h = flow of heat, with units of [J/s = W]
k_t = *thermal conductivity* of the rock, with units of [$W \cdot m^{-1} \cdot K^{-1}$]
A = cross-sectional area of the rock core, with units of [m^2]
T_i , T_o = inlet/outlet temperatures, with units of [K]
L = length of the core, with units of [m]

This equation can be thought of as providing a definition of thermal conductivity. It tells us that the conductive flow of heat is proportional to the area, and proportional to the temperature gradient, *i.e.*, the temperature drop per unit length, $\Delta T/L$. The constant of proportionality is the thermal conductivity.

Fourier's law is mathematically analogous to Darcy's law, with the flow of heat Q_h being analogous to volumetric fluid flow Q, temperature drop ΔT analogous to pressure drop ΔP, and thermal conductivity k_t analogous to the ratio of permeability/viscosity k/μ (*i.e.*, the mobility) (compare with equation 1.2.1).

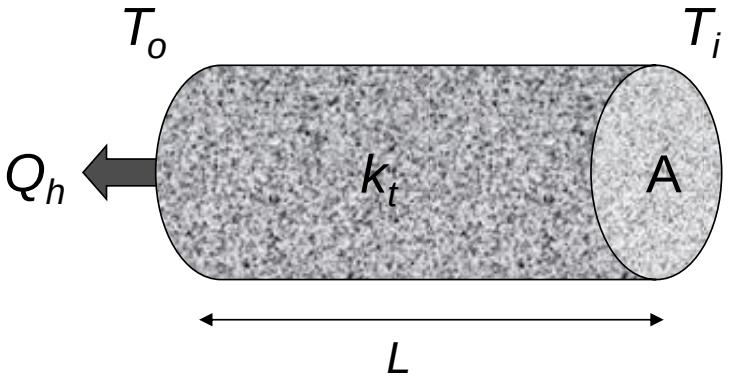

Figure 3.1.1. Conductive heat flux through a cylindrical conductor of length L, area A and thermal conductivity k_t.

Similar to Darcy's law, it is usually more convenient to work with the heat flow per unit area (often termed the heat flux), $q_t = Q_h/A$. Fourier's law is therefore usually written as

$$q_h = \frac{Q_h}{A} = \frac{k_t(T_i - T_o)}{L} = k_t \frac{\Delta T}{L} \qquad (3.1.2)$$

where the heat flux q_t has units of [W·m^{-2}]. Similar to Darcy's Law, we can also define Fourier's Law at a point for heat flow in a given direction

$$q_{hn} = -k_t \frac{dT}{dn} \quad (3.1.3)$$

where n denotes the direction of heat flow (x, y or z).

The above equations assume that the thermal conductivity is the same in all directions. But in most reservoirs, the conductivity in the horizontal plane (parallel to bedding) is different to that in the vertical plane (perpendicular to bedding). The conductivities in different directions within the horizontal plane may also differ, but this difference is usually not as great as between horizontal and vertical heat flow. Similar to permeability, thermal conductivity is anisotropic (e.g. Fig. 1.2.2).

If the rock is anisotropic, eq. (3.1.3) does not hold in an *arbitrary* direction, even if we use an appropriate value of k_t. The correct version of Fourier's law for an anisotropic rock must be written in terms of the *conductivity tensor* which, similar to permeability, is a symmetric 3x3 matrix that has six independent components.

The range of values of thermal conductivity for reservoir materials is much smaller than the range of permeability (see Table 1.2); the lowest value of thermal conductivity is typically given by water (k_t of order 0.6 W·m^{-1}·K^{-1}) and the largest value by the common rock forming mineral quartz (in its crystalline form, k_t is of order 8 W·m^{-1}·K^{-1}). Typical reservoir rock thermal conductivities are of order 2-4 W·m^{-1}·K^{-1}.

3.2 Heat capacity

The specific heat capacity of a material relates the heat energy gained or lost to the temperature change of a unit mass of the material. For a mass m of a material, the change in energy ΔQ is related to the change in temperature ΔT by

$$\Delta Q = mc_p \Delta Q \quad (3.2.1)$$

where c_p is the specific heat capacity in units of J·kg^{-1}·K^{-1}. The heat capacity is an important property in geothermal and thermal energy storage reservoirs because it relates changes in temperature and energy. The heat capacity may also be expressed as the volumetric heat capacity, which relates the heat energy gained or lost to the temperature change of a unit volume of the material, or the molar heat capacity, which relates the heat energy gained or lost to the temperature change of one mole of the material. The volumetric heat capacity has units of J·m^{-3}·K^{-1}, while the molar heat capacity has units of J·mol^{-1}·K^{-1}. Similar to reservoir thermal conductivity, the heat capacity of a reservoir is a function of the rock heat capacity, and the heat capacity of the fluid(s) saturating the pore space.

The specific heat capacity of a substance, especially a gas, may be significantly higher when it is allowed to expand as it is heated (specific heat capacity at constant pressure) than when it is heated in a closed vessel that prevents expansion (specific heat capacity at constant volume). These two values are usually denoted by c_p and c_v respectively and their ratio $\gamma = c_p/c_v$ is the heat capacity ratio.

The term specific heat is sometimes used to relate the refer to the ratio between the specific heat capacities of a substance at a given temperature and of a reference substance at a reference temperature such as water at 15°C.

3.3 Measurement of thermal properties

3.3.1 Measurement of thermal conductivity

There are broadly two approaches to measure thermal conductivity. The first is to measure the thermal conductivity of the reservoir rock(s) of interest, saturated with the fluid(s) of interest, ideally at the conditions of interest for the geoenergy application under consideration. The second is to measure the conductivity of 'dry' samples and combine dry rock and fluid conductivities to estimate the saturated rock conductivity.

Measurements of both dry and saturated rock sample conductivities can be subdivided into three approaches: steady state methods, unsteady state (transient) methods, and optical methods. Steady state and transient methods use equipment designed to allow Fourier's law to be applied for steady linear or radial heat flow, or transient linear or radial heat flow, whilst minimising heat losses and transport by fluid convection.

3.3.1.1 The Divided Bar Method

The divided bar method is a steady-state comparative method in which the temperature drop across a disk of rock is compared with that across a disk of standard material of known conductivity (Figure 3.3.1). Rock samples are typically 30 to 50mm in diameter and 10 to 30mm in thickness. The samples are saturated with the fluid of interest and held in place under an axial load of 4 to 6 MPa ensuring that microcracks are closed or fluid saturated. Most modern DBs operate on the principle of constant temperature drop and reach steady-state conditions very quickly. A measurement can be completed in 10 to 15 minutes. The geometry approximates steady 1D heat flow as described by Fourier's Law, minimizing radiative losses, convection of fluids and contact thermal resistance. To explore anisotropy in thermal conductivity requires several disks to be cut from the same sample, relative to the bedding planes.

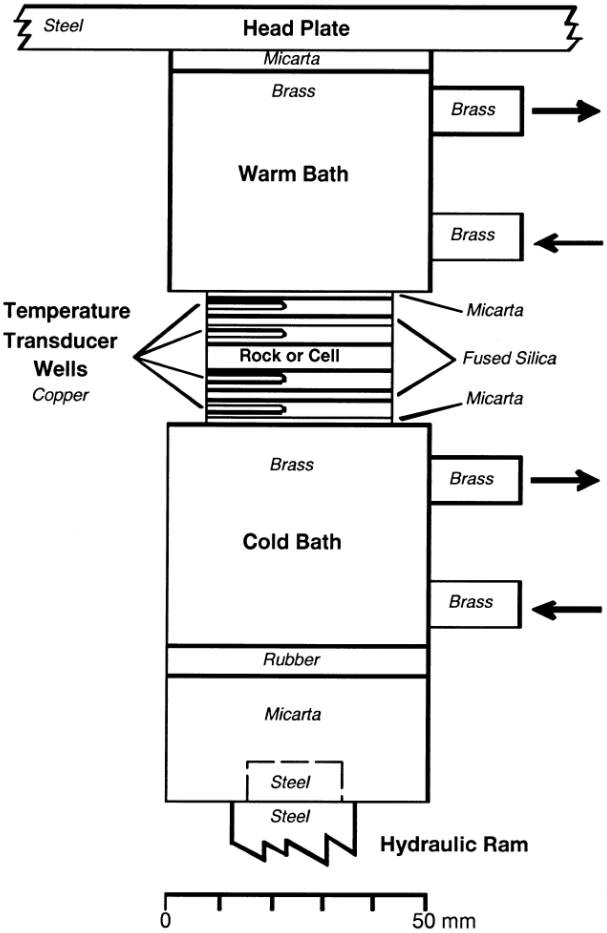

Figure 3.3.1. Divided bar apparatus for measuring thermal conductivity.

3.3.1.2 Transient Line Source Method

This method is based on the theory of a line-source in an infinite medium. The apparatus used is typically a half-space line-source comprising a needle probe embedded in and flush with the surface of a material of very low thermal conductivity. Samples may be dry or saturated. The requirement of an infinite probe length is realized if the length-to-diameter ratio of the needle probe is larger than 30:1 and if the probe temperature is recorded at the centre of the probe. Rotating the line source with respect to the bedding allows the main thermal conductivity components to be determined. An electrical current is applied to the probe to cause heating and the temperature change is measured and interpreted using Fourier's Law for transient, radial heat flow. Measurements are rapid (seconds to minutes) but can suffer from contact thermal resistance, and the lack of pressure may allow microcracks to remain open. Because the temperature changes during measurement, transient methods are more susceptible to variations in heat capacity and care must be taken to avoid excessive heat losses by, for example, using a sample that is too thin or small.

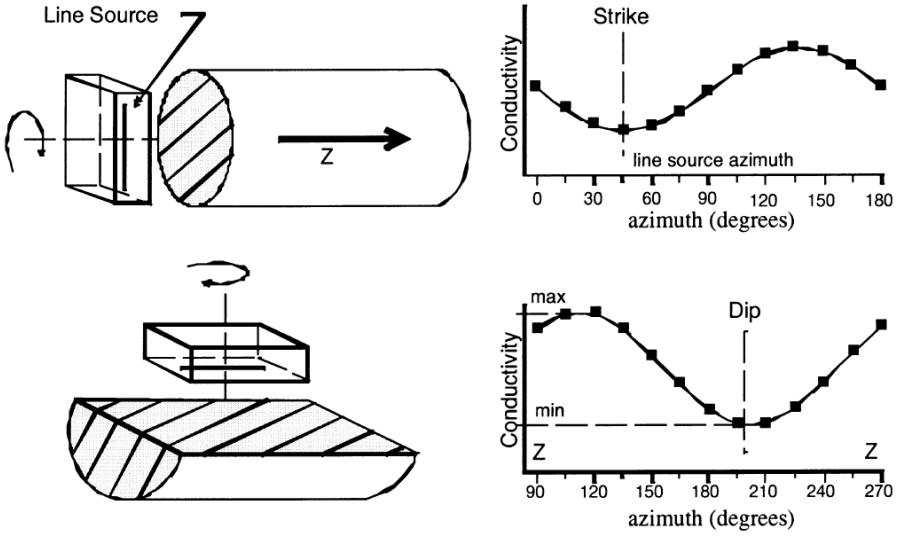

Figure 3.3.2. Determination of main thermal conductivity components with a half-space line-source.

3.3.1.3 Transient Plane Source Method

The probe is here engineered to approximate a plane source, rather than a line source (Figure 3.3.3). The sample is cut into two pieces and the probe is placed between the pieces. An electrical current is applied to the probe to cause heating and the temperature change is measured and interpreted using Fourier's Law for transient, linear heat flow. Measurements are rapid (seconds to minutes) but can suffer from contact thermal resistance. Care must be taken to avoid heat losses by, for example, using a sample that is too thin or small. Several repeat measurements may be required.

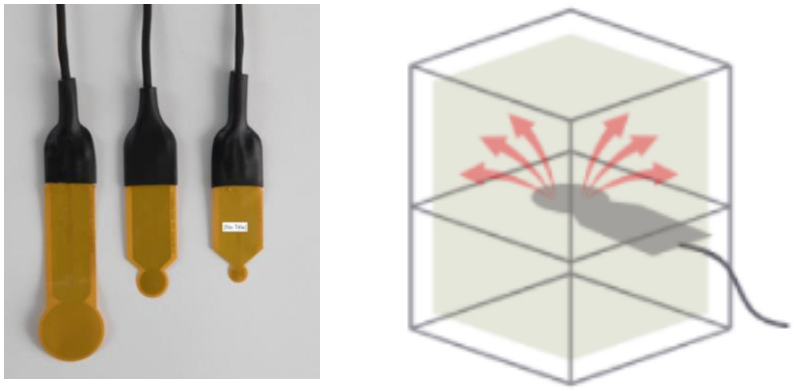

Figure 3.3.3. Transient plane source probes and application.

In the modified transient plane source, a guard ring surrounds the mean sensor coil to minimize radial heat flow and ensure the geometry more closely approximates transient 1-D heat flow (Figure 3.3.4).

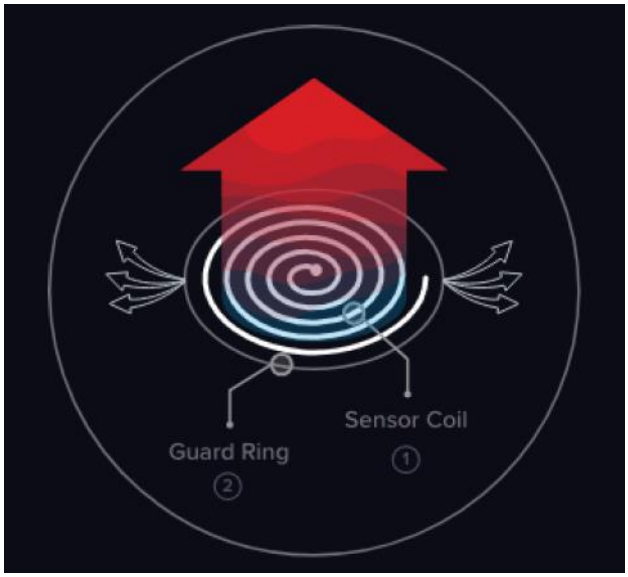

Figure 3.3.4. Modified transient plane source probe with guard ring.

3.3.1.4 Optical Method

The Optical Scanning Method is relatively new to Earth science. The theoretical model is based on scanning a sample surface with a focused mobile and continuously operated constant laser heat source in combination with an infrared temperature sensor (Figure 3.3.5). The heat source and sensor move with the same speed relative to the sample and at a constant distance from the sample. The temperature sensor displays the value of the maximum temperature rise along the heating line behind the source. The maximum temperature rise T_{max} is given by

$$T_{max} = \frac{Q}{2\pi x k_t} \tag{3.3.1}$$

where k_t is the thermal conductivity, Q is the source power and x is the distance between source and sensor. If the samples under study and a reference standard with known conductivity are aligned along the scanning direction, the thermal conductivity of each sample can be determined from the ratio of temperature rise between the sample and the standard. Samples may be dry or saturated.

3.3.2 Combining dry rock and fluid conductivities to estimate the saturated rock conductivity

Combining measurements of dry rock conductivity and fluid conductivity in the absence of a detailed pore-scale model requires significant simplification of the rock and fluid geometry. It is assumed that the rock and fluids form layers and that heat flow is either parallel or perpendicular to the layers, to give upper and lower bounds on the saturated rock conductivity (Figure 3.3.6). The upper bound is then given by the arithmetic average, assuming that heat flow is parallel to layers, and the lower bound is given by the harmonic average, assuming heat flow is perpendicular to layers

$$\text{Arithmetic average } k_r = \emptyset k_f + (1-\emptyset)k_s \tag{3.3.2}$$

$$\text{Harmonic average } k_r = \frac{\emptyset}{k_f} + \frac{(1-\emptyset)}{k_s} \tag{3.3.2}$$

where ϕ is the porosity, k_f is the fluid conductivity and k_s is the dry rock conductivity.

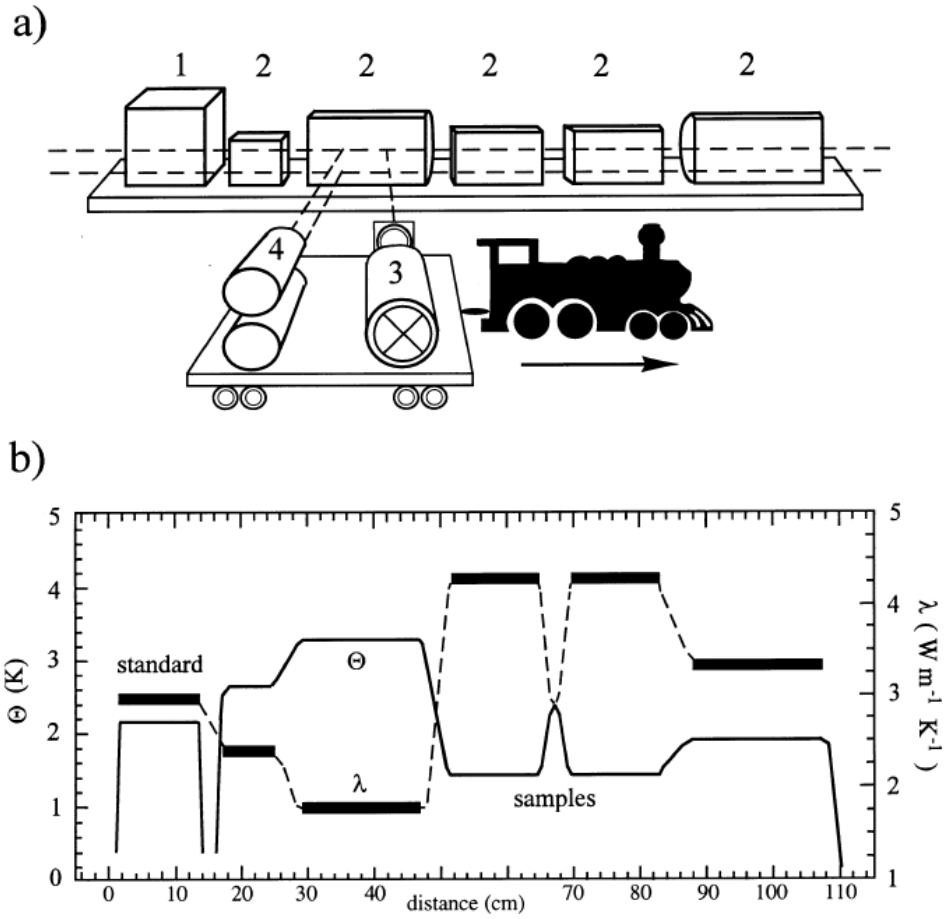

Figure 3.3.5. Schematic of optical scanning apparatus. (1) standard with known thermal conductivity; (2) samples; (3) laser heat source; (4) infrared radiometers. Below shows example measured temperature (θ) and thermal conductivity (λ).

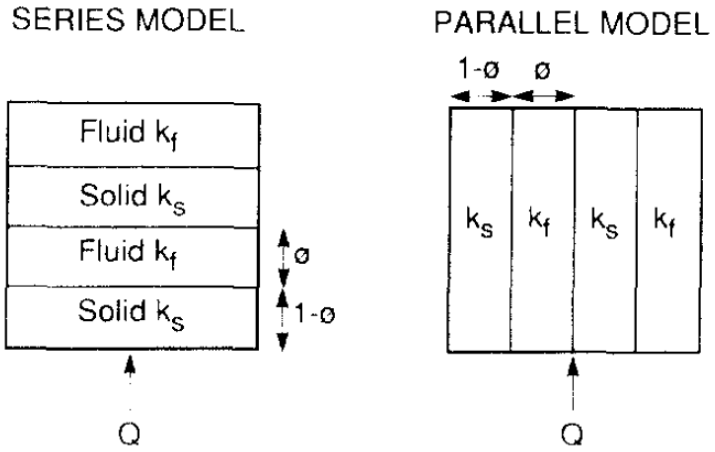

Figure 3.3.6. Assumed geometry of rock and fluid layers for simple averaging.

Zimmerman (1989) showed that tighter constraints can be placed on the maximum and minimum values of effective thermal conductivity using the Hashin and Shtrikman bounds, given by

$$k_f + \frac{3k_f(k_s-k_f)(1-\emptyset)}{3k_f+(k_s-k_f)\emptyset} \leq k_r \leq k_s + \frac{3k_s(k_f-k_s)\emptyset}{3k_s+(k_f-k_s)(1-\emptyset)} \qquad (3.3.3)$$

3.3.1 Measurement of heat capacity

Heat capacity can be measured using a calorimeter, in which a known amount of heat is added to a sample and the change in temperature is added (e.g. Figure 3.3.6). Transient methods to measure thermal conductivity can also be extended to report heat capacity.

The heat capacities of all common rock forming minerals and many rocks have been determined (e.g. Figure 3.3.7) and, unlike thermal conductivity, the effective heat capacity of a saturated reservoir rock can be calculated using a simple weighted arithmetic average of the heat capacities of the rock and fluid(s), or mineral(s) and fluid(s). For example, if the specific heat capacities of the fluid and rock are known, then the volumetric heat capacity (for example) can be calculated using

$$k_r = \emptyset \rho_f c_{P,f} + (1 - \emptyset) \rho_p c_{P,p} \tag{3.3.4}$$

where ϕ is the porosity, ρ_f is the fluid density, ρ_p is the dry rock density, $c_{P,f}$ is the specific heat capacity of the fluid, and $c_{P,p}$ is the specific heat capacity of the dry rock.

Extending this approach. $c_{P,p}$ can be calculated from modal mineral data and individual mineral c_P values by taking the appropriate weighted average

$$C_{P,p} = \frac{\sum_{i=0}^{n} V_i \rho_i c_{P,i}}{\sum_{i=0}^{n} V_i \rho_i} \tag{3.3.5}$$

where V is the volume of mineral i in the sample, and ρ_i is the density of mineral i.

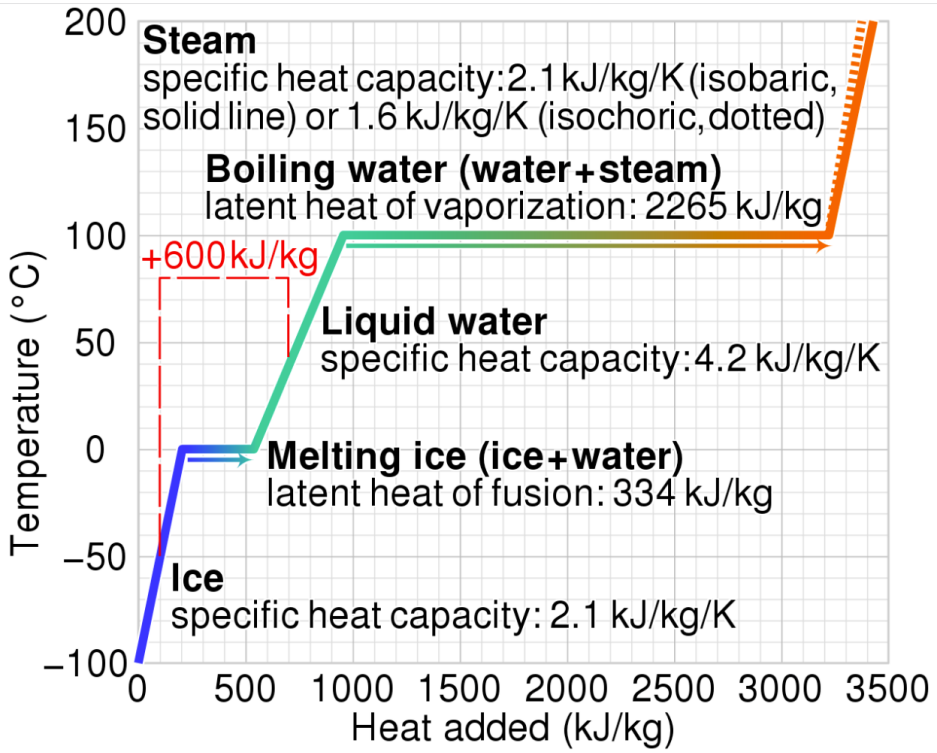

Figure 3.3.5. Calorimeter data for pure water.

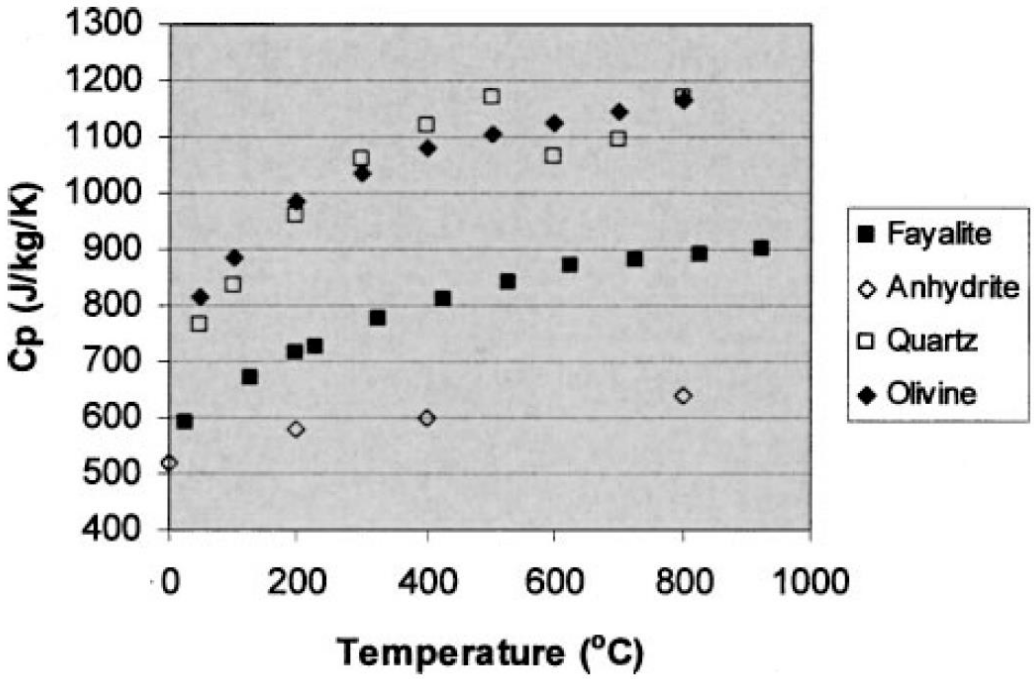

Figure 3.3.6. Specific heat capacity data for some common minerals.

4. Core sample acquisition, handling and preparation

4.1 Reservoir Samples

Reservoir rock samples are divided into two subgroups: (1) drill cuttings and (2) core samples (Fig. 4.1.1; 4.1.2).

4.1.1 Drill Cuttings

Drill cuttings are circulated by drilling mud and are collected at the surface for examination. They provide useful information on layers penetrated in the subsurface, such as mineralogical composition and pore size distribution of the rock, and possible fluid content of the layers. Although they provide timely and relatively inexpensive data, reliability and accuracy of information derived from drill cuttings are limited. One of the uncertainties is associated with the depth. The cuttings travel to the surface with the mud, which may take a few hours as the travel time depends upon the friction of the cuttings in the mud and the circulation hydraulics.

Figure 4.1.1. Typical plugs used in core analysis.

Figure 4.1.2. A short section of whole core, showing where plugs have been drilled out.

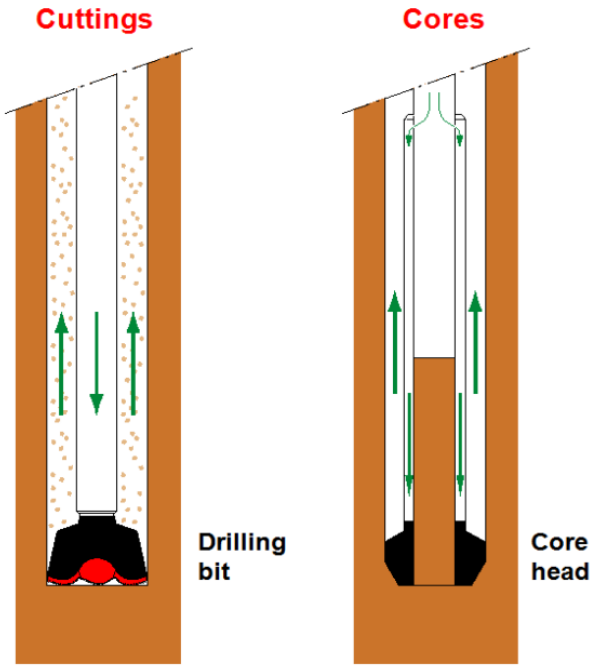

Figure 4.1.3 Schematic of reservoir rock sampling. Drill cuttings (left) and core sample (right).

Therefore, sample depth is often not very accurately defined. Another shortcoming is associated with the size and irregular shapes of the cuttings. As the cuttings are small and have been disturbed by the drill bit, accurate quantitative petrophysical measurements like porosity and permeability may not be possible. In addition, the cuttings are often contaminated by the drilling mud. This can significantly modify the sample state away from that of the reservoir. However, the information obtained through cuttings can be complementary to that produced by the more accurate and sophisticated evaluation methods of core plug analysis.

4.1.2 Coring

There are two main types of coring: (1) coring axial to the well bore, termed *bottomhole continuous coring*, and (2) coring from sidewall of the borehole, termed *sidewall coring*.

4.1.2.1 Bottomhole Continuous Coring

As the name suggests, this method cuts the core at the bottom of the borehole, axial to the well bore. Bottomhole continuous cores are obtained using a core barrel attached to the bottom of the drill pipe. A coring bit is attached to the outer barrel and a core catcher is fitted to the bottom of the inner barrel. A schematic of the core barrel and coring bit is shown in Figure 4.1.4. A cylindrical piece of reservoir rock, which is often 9 or 18 m in length and 5-8 cm in diameter, is forced into the core barrel and taken to the surface (Fig. 4.1.5). Although it is possible to cut the core at different lengths and diameters, a reduction in core diameter leads to faster and hence cheaper coring operations.

It is also possible to cut oriented cores, which have lines scribed along their length to show the core position relative to the core head. Oriented cores are particularly valuable to assist in the interpretation of sedimentary structures such as cross-bedding, and where fractures are present to help determine fracture orientation. Standard coring techniques have been utilized with varying success, as they suffer from a number of limitations. Damage of the core material (especially for unconsolidated reservoirs), mud invasion, and high costs associated with some coring operations, are major issues confronting core analysis.

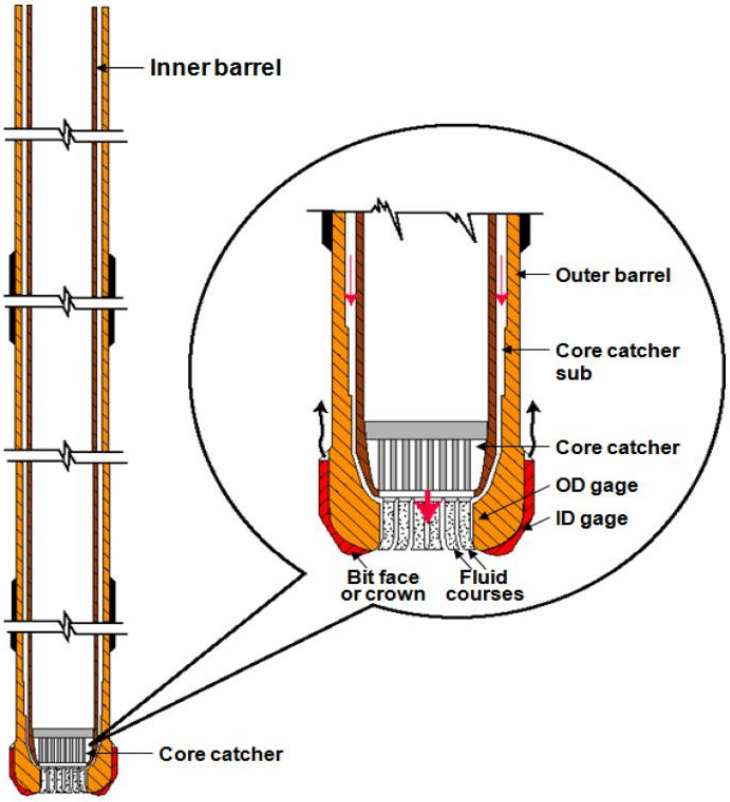

Figure 4.1.4 Schematic showing the core barrel and the bit attached to the bottom of the drill pipe.

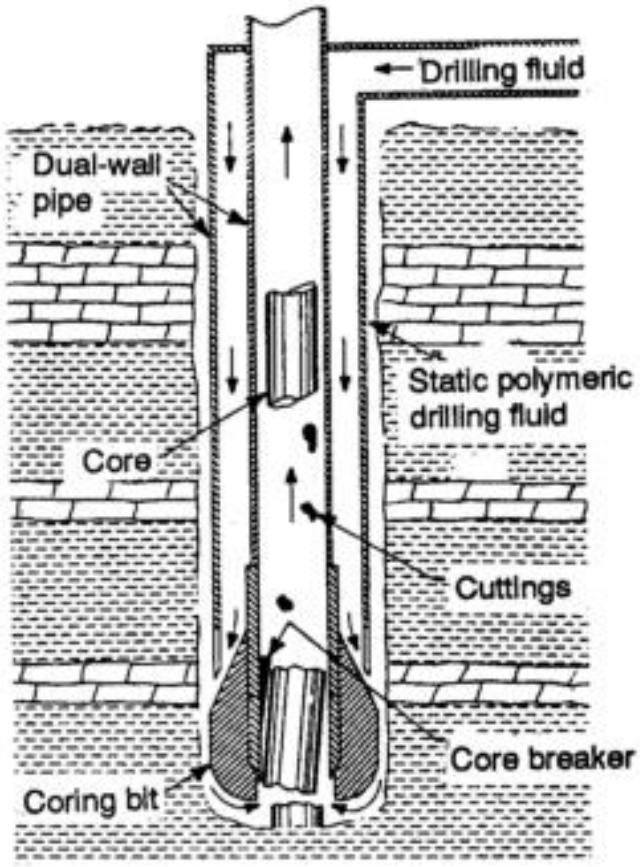

Figure 4.1.5 Schematic showing recovery of core to surface.

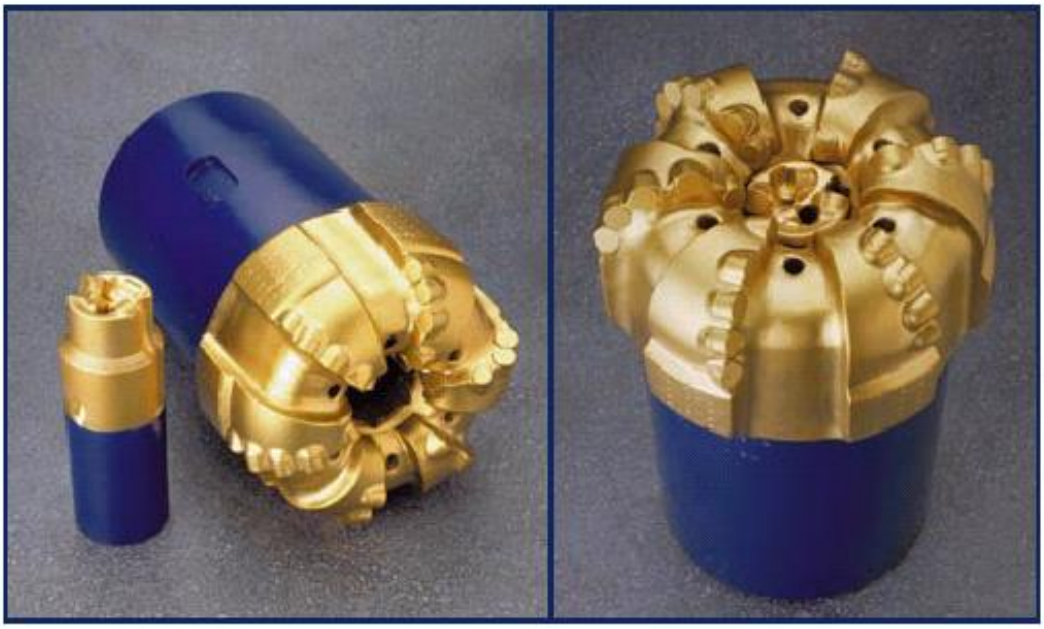

Figure 4.1.6 Drill bits for coring.

The coring-while-drilling (CWD) system is designed to provide operators with the flexibility of bottomhole coring or drilling with the same bit, without tripping-out of the borehole. In the drilling mode, the system is used in the same manner as a conventional bottomhole assembly. In the coring mode, a drill bit plug is replaced with an inner barrel and bearing assembly that transforms the drill bit into a core bit. After core recovery, the coring assembly is retrieved. A coring-while-drilling system significantly reduces the time and therefore the cost necessary to cut continuous full-diameter cores.

4.1.2.2 Sidewall Coring

Sidewall sampling is another means of obtaining reservoir rock samples if borehole conditions do not allow full-diameter continuous coring. It is also cheaper than continuous axial coring. Rock samples are obtained either by firing hollow cylindrical bullets into the borehole wall, which is called percussion sidewall coring, or by drilling a small horizontal core in the same way that plugs are cut from full-diameter core, which is called rotary sidewall coring. Figure 4.1.7 shows the schematics of a sidewall sample gun, which is used to obtain percussion sidewall cores, and Figure 4.1.8 shows a rotary sidewall coring tool. The advantages of this technique to obtain sidewall core material are (i) it is quick and relatively inexpensive, (ii) the exact depth of coring is known and (iii) recovered samples are much larger than drill cuttings, which enable better evaluation of geological variations and quantitative petrophysical analysis. Disadvantages of sidewall coring are (i) samples (especially percussion cores) are often damaged so they may be unsuitable for laboratory tests and (ii) volumes are usually insufficient for performing advanced core measurements.

4.2. Core Handling and Preservation

The main objective of a coring and core preservation program is to obtain rock that is representative of the reservoir and deliver it to the core analysis laboratory in as close to the reservoir state as possible. Although a variety of techniques have been developed, there is no single best method for handling and preserving core samples. Different rock types may require additional precautions. The most appropriate core handling techniques may depend on the length of time for transportation, storage and the nature of the specific tests to be conducted.

Conventional core handling involves breaking lengths of core into 1m (~3 ft) sections as the core is retrieved from the inner barrel onto the drill floor or catwalk. These pieces are then loaded in

sequential order into transit core boxes and taken to the place designated for core layout and description. The core should be laid-out, cleaned, fitted, marked and described, and then packed into the final transport boxes for shipment to the core storage/analysis facilities.

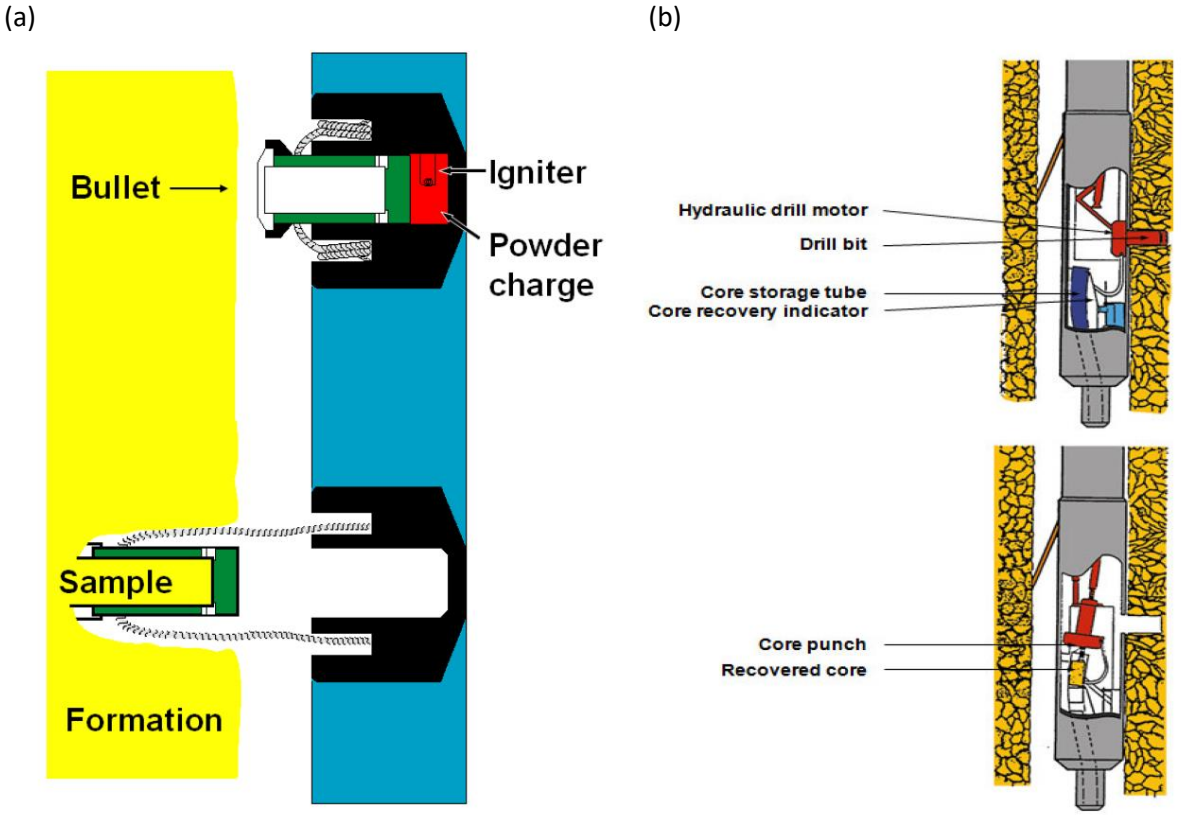

Figure 4.1.7 Schematic of (a) a sidewall sample gun which is used to obtain percussion sidewall cores, and (b) a rotary sidewall coring tool.

Containerized cores, however, need certain additional precautions to prevent/limit core disturbance. Flexure of inner barrels has been shown to induce significant core damage through cracking. This problem is especially marked for the smaller diameter barrels and is more pronounced for fibreglass and plastic liners than it is for other more rigid materials. In order to limit this disturbance, it is essential that the inner barrels/liners are supported with rigid structural supports. Core cradles designed to hold 9m (~30 ft) lengths of inner barrel are considered to be the optimal solution for this purpose in terms of preventing flexure whilst safely lifting the core. The core can then be processed (e.g. measuring, plugging, cutting, sampling, repacking) according to the previously agreed programme.

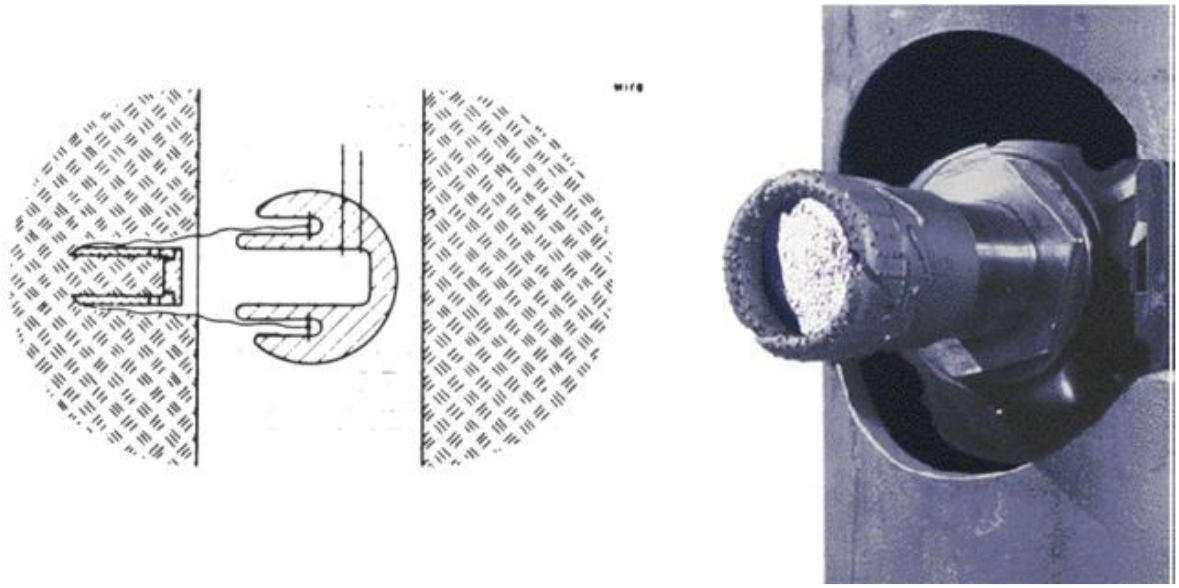

Figure 4.1.8 A rotary sidewall coring tool.

Unconsolidated core normally requires some form of stabilization inside the core barrels prior to transport. Two stabilization methods are in general use in the industry: (i) freezing of the core and (ii) injection of fast hardening epoxy resin/plastics in the core/core barrel annulus. Often a combination of both methods is used. Figure 4.2.1 gives an overview of core handling procedures for unconsolidated rocks.

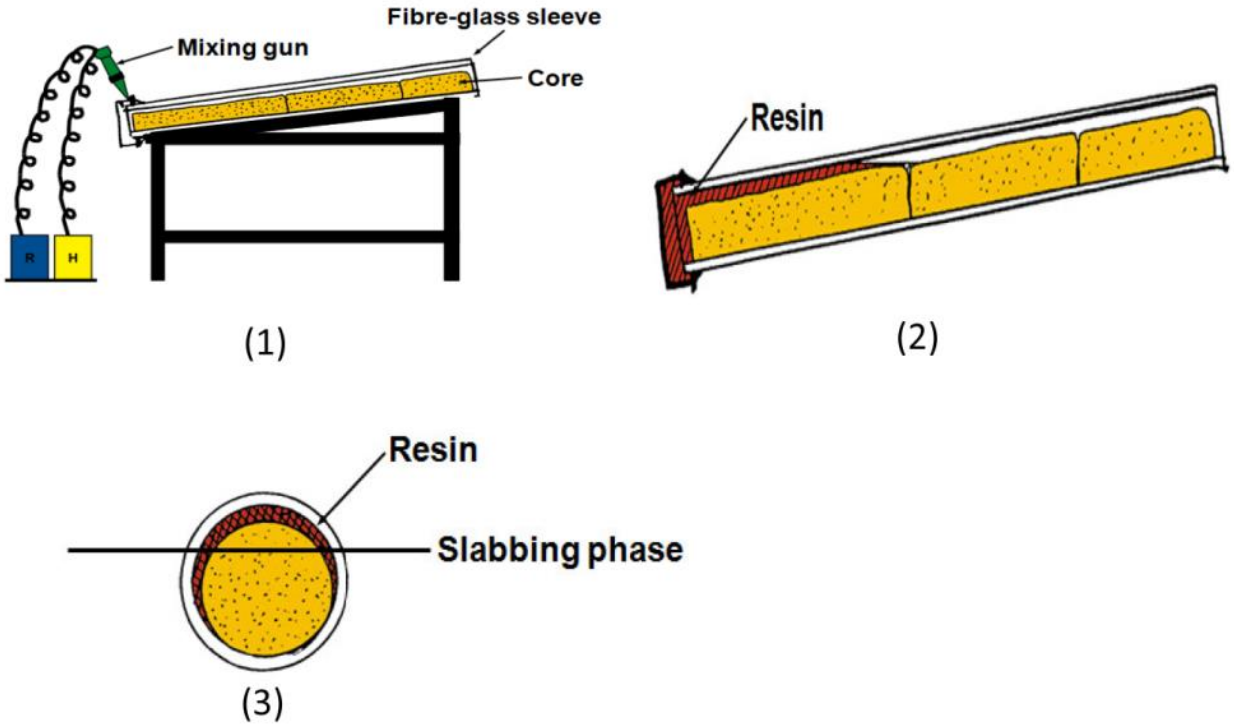

Figure 4.2.1. An overview of core handling for unconsolidated core samples: (1) injection of fast hardening plastic (resin), (2) resin fills the core and annulus, and (3) slabbing takes place.

4.3. Core Analysis Preparation

After the core has been cut and preserved at the well site, it is transported to the core analysis laboratory where it is subject to a wide variety of measurements. However, several steps should be taken before these measurements are obtained. These are imaging, sample selection, core plugging and plug preparation.

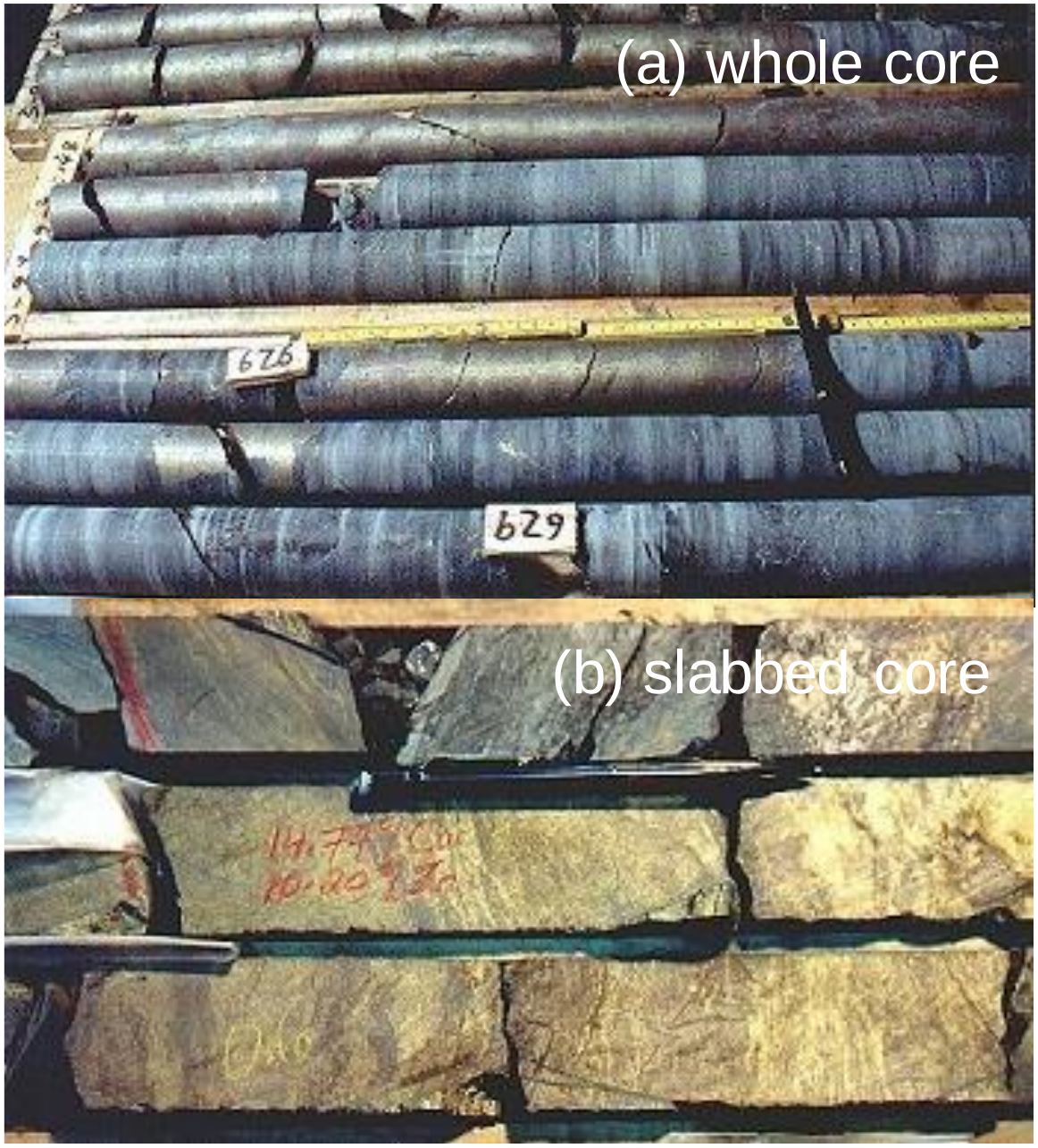

Figure 4.2.2. Examples of (a) whole core and (b) slabbed core.

4.4 Core Description and Imaging

Once the core is retrieved to the surface, gamma ray logging is performed as the first step towards core analysis. The core gamma ray logger is a portable device that provides gamma ray logs immediately after the core has been cut and retrieved to the surface. This analysis can be conducted either at the well site or in the laboratory. The main purpose is to (i) correlate the depth of the cored sections with wireline measured depth (which is considered to be definitive) by comparison of core- and wireline gamma ray logs over the same interval, and (ii) interpret anticipated lithology by, for example, delineating mudstone sections from non-mudstone (reservoir) intervals. Reliable on-site analysis enables operators to make rapid, real-time decisions on further coring, testing and well completion activities.

X-ray computed tomography (CT) is one of the most widely used imaging techniques, which permits visualization of internal rock features. CT scanners used in core petrophysics are modified from medical CT scanners. A CT scanner is a non-destructive imaging tool which allows a core to

be scanned whilst still contained in the fibreglass barrels and the plastic liner materials. It reveals not only the internal structures of the core but also the damage done by various coring and core handling actions prior to the laboratory measurements. The results can be used to determine slabbing directions or even optimize the planning of core plug positions. Furthermore, a statistically representative sampling strategy is required for heterogeneous reservoirs where CT scanning can be used to assess the degree of heterogeneity. Figure 1.4.1 shows a schematic of computer-aided scanning of a core material using X-ray tomography, and CT images obtained from a whole core scanning study.

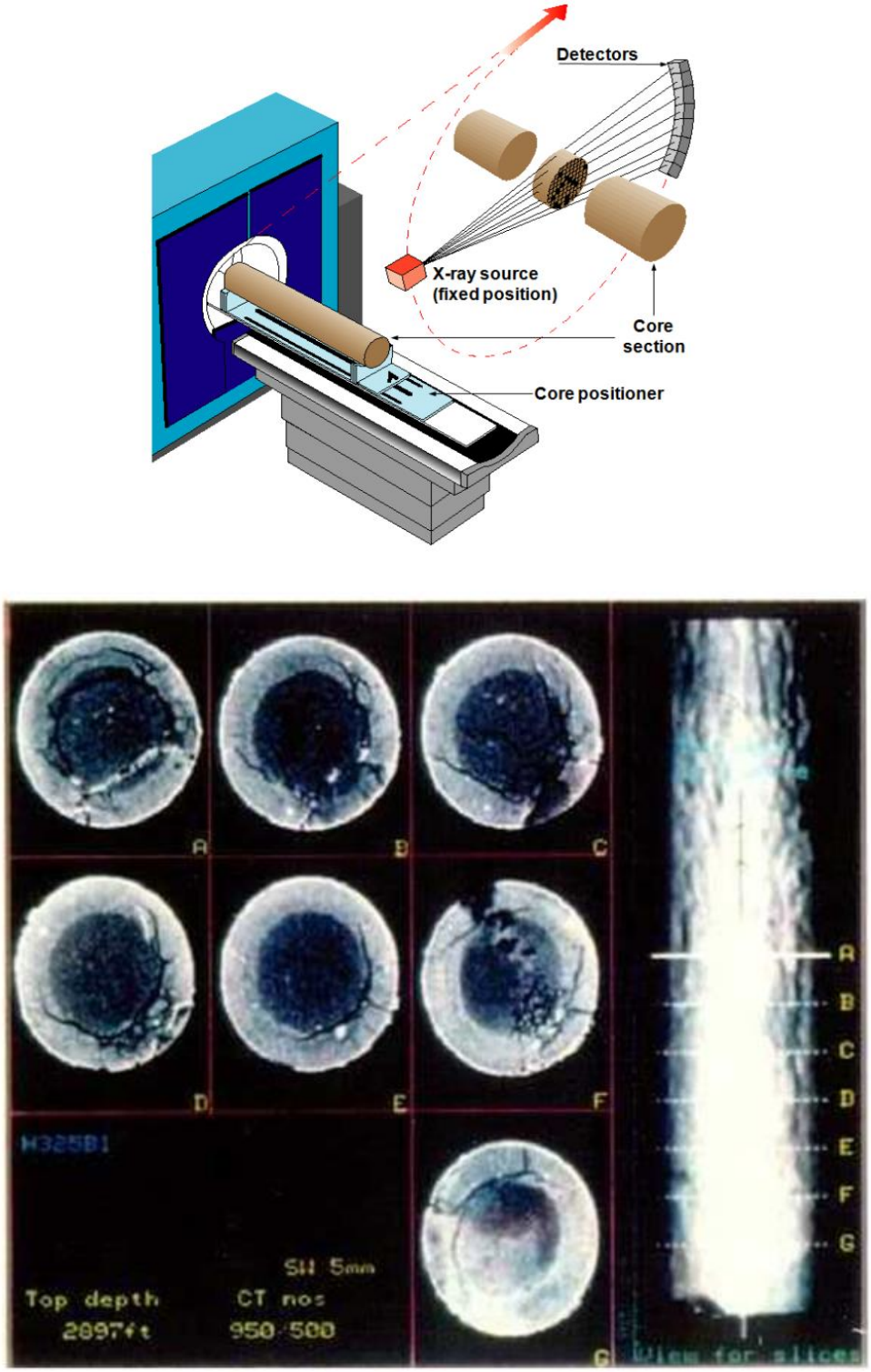

Figure 4.4.1 Schematic of computer aided scanning of core material (above) and CT images obtained from a whole core scanning study (below).

4.5 Sample Selection

Core sampling has a significant influence on the success of core analysis laboratory measurements. A poorly conducted sampling program may limit the scope and result in ineffective experimental measurements. Sample selection must serve the needs of different disciplines such as geology, petrophysics and reservoir engineering. Ideally, sampling should result in a statistically meaningful representation of the core material. Sample selection varies depending on the type of test. As the requirements of basic and advanced core analysis differ significantly, sample selection should be done accordingly to meet the overall core analysis objectives.

4.5.1 Basic Core Analysis Sampling

Ideally, basic core analysis for porosity and permeability is done on plugs obtained every foot (~30 cm) along the cored section. If too many plugs fall in regions of poor-quality core material, plugs may be taken at different positions (a few inches away from the predetermined locations). In general, emphasis should be paid to the cutting of plugs as close to uniform spacing as possible without any regard for variations in lithology. Otherwise, a bias towards apparently better reservoir properties may be unwittingly introduced, which can lead to statistically unrepresentative core data and improper log calibration. However, plugs which contain two different lithologies (i.e. which lie on the boundary of different lithologies) should be avoided, as the experimental data obtained on these core plugs can be misleading. Core plugs can be cut both in parallel and perpendicular orientations to bedding, to help evaluate anisotropic reservoir parameters such as permeability (e.g. Fig. 4.5.1).

Fig. 4.5.1. Plugs drilled perpendicular to bedding in a heterolithic (mixed sandstone-mudstone lithology) core. Each plug samples a mixture of sandstone (pale) and mudstone (dark).

4.5.2 Advanced Core Analysis Sampling

As the name suggests, some special precautions should be taken while sampling for advanced core analysis laboratory measurements. Advanced core analysis would include measurement of electrical and thermal properties, and also multiphase flow properties such as relative permeability and capillary pressure, especially at reservoir conditions. You will return to multiphase flow properties in a later course. Unlike basic core analysis, samples are not taken at regular intervals for advanced measurements. Sampling often focusses on particular rock types within the reservoir. The location and number of samples chosen for these measurements should be representative of the rock type under consideration. A core that first appears completely uniform may actually be highly heterogeneous with respect to petrophysical parameters. Therefore, while making the sample selection, use of a non-destructive imaging technique such as CT scanning is highly recommended. The number of advanced core analysis samples is usually much smaller than in basic core analysis.

4.6 Plug Preparation

As mentioned in the previous sections, plug selection is dependent on the type of measurements to be conducted. For basic core analysis, plugging is performed every foot (~ 30 cm); however, in advanced core analysis, emphasis is on rock types. Between the time plugs are drilled and core analysis measurements begin, several preparation steps should be taken such as cleaning, saturation measurement and drying.

4.6.1 Plug Drilling

A whole core is ‘slabbed’ along its long axis into two pieces. Prior to slabbing, selected sections of the core may be preserved for whole core analysis or for certain experiments. The optimum slab plane is usually determined via CT scanning. The slabs are usually cut at 1/3 and 2/3 of the core diameter along its long axis. Plugs are cut from the thicker section (the 2/3 piece). While drilling plugs, various lubricants are used depending on the core material. Fresh water is used for clean sands and carbonates. Kerosene (or Blandol) is used for shale and halite bearing samples to avoid damaging the clay minerals in the shale or dissolving out the halite. Brine is used for cores containing clays or from high salinity environments.

Unconsolidated cores are often kept frozen and plugs are drilled using liquid nitrogen. Plugging usually takes 10-15 minutes per piece. Fluid flow properties may vary with sample orientation. Therefore, care needs to be taken in selecting the direction of bedding. Horizontal plugs should be drilled parallel to the apparent bedding plane; vertical plugs are drilled perpendicular to the apparent bedding plane.

4.6.2 Plug Cleaning

Before porosity and permeability measurements take place, samples should be thoroughly cleaned of reservoir fluids. Cleaning is often achieved using a hot solvent extraction (‘Soxhlet’) technique. The most appropriate solvent depends on rock type, fluid characteristics, rock mineralogy, and timing. Toluene is the most commonly used solvent to extract water and hydrocarbons. It is usually followed by extraction of any salts with a chloroform/methanol mixture. The Soxhlet technique removes all the fluids from the core.

Figure 4.6.1 shows a schematic of the Dean-Stark apparatus. The sample is first weighed and placed into the apparatus. Solvent is vaporized by boiling and rises up to extract the water from the sample. Solvent and water vapours then condense in a reflux-type condenser and are collected in a calibrated receiving tube. Water is immiscible with the solvent and settles at the bottom of the tube, as it is the denser phase. Therefore, the extracted volume of water can be measured directly in the receiving tube. The solvent refluxes into the distillation flask. Any extracted oil remains in solution.

4.6.3 Drying

After the saturation measurement is conducted and cleaning is performed, the core is dried. Prior to porosity and permeability measurements, all the remaining solvent and salt (deposited from the saline formation water during extraction) must be removed. There are several drying techniques; oven drying is the most common, because it is quick and inexpensive. Multiple core plugs can be simultaneously dried in a vacuum convection oven. The temperature is set at around 95 ºC and each core sample should be dried until constant weight is obtained. When hydrated minerals such as clays are present, humidity ovens may be used to minimize sample alteration. Humidity ovens can be set at 60°C and 40% relative humidity. Because of the low temperature, drying may take several days. The resulting 'effective' porosity needs careful calibration to log-derived effective or total porosity.

If a rock contains minerals such as hairy illite (a type of clay mineral), which are sensitive to fluid phase changes, a 'critical point drying' (CPD) technique may be employed. These minerals can be 'damaged' due to the large interfacial forces that can be created in very small cavities as the 'drying front' proceeds into the sample. The CPD technique prevents the development and advancement of a gas-liquid or liquid-liquid interface within the rock by raising the fluid above its critical point.

In order to investigate the drying effects, scanning electron microscopy (SEM) is generally used in conjunction with CPD. This technique is usually slow as it depends on the diffusion time, which is a function of sample size, permeability and fluids initially in place. Critical point drying can take from 2 weeks to 2 months.

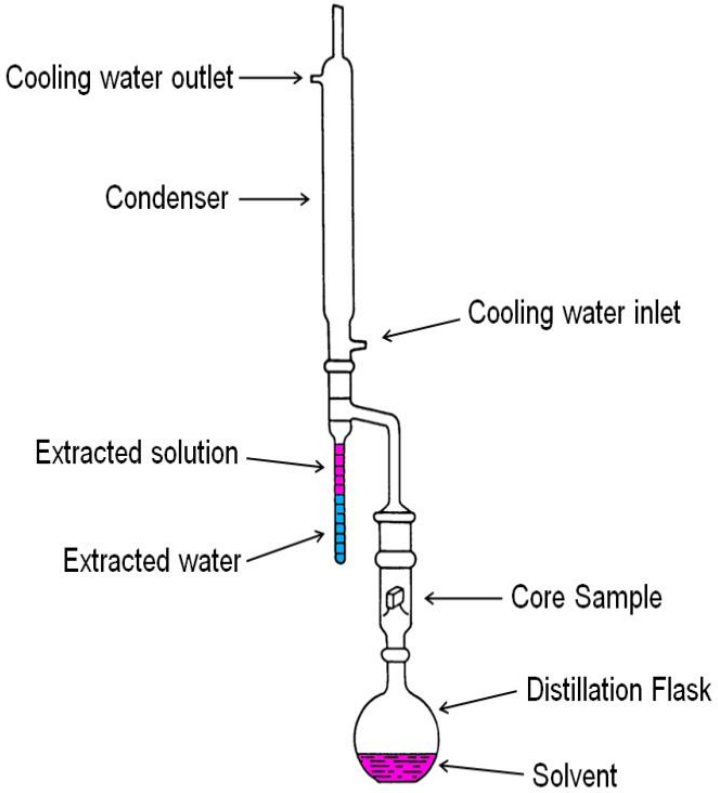

Figure 1.6.1 Dean-Stark distillation extraction apparatus.